

**TECHNISCHE UNIVERSITÄT MÜNCHEN**

**Pankreas-Forschungslabor  
Chirurgische Klinik und Poliklinik  
Klinikum rechts der Isar**

**Pigment Epithelium-Derived Factor Increases Neuropathy and  
Fibrosis in Pancreatic Cancer**

**Tamar Samkharadze**

Vollständiger Abdruck der von der Fakultät für Medizin der Technischen Universität München zur Erlangung des akademischen Grades eines Doktors der Medizin genehmigten Dissertation.

Vorsitzender: Univ.-Prof. Dr. E. J. Rummeny

Prüfer der Dissertation:

1. apl. Prof. Dr. J. H. Kleeff
2. Univ.-Prof. Dr. F. R. Greten
3. Univ.-Prof. Dr. J. Schlegel

Die Dissertation wurde am 02.03.2011 bei der Technischen Universität München eingereicht und durch die Fakultät für Medizin am 07.03.2012 angenommen.

## TABLE OF CONTENTS

ABBREVIATIONS	5
1. ABSTRACT	8
2. INTRODUCTION	9
2.1. Pancreatic Cancer Epidemiology and Clinical Presentation	9
2.2. Abundant Dense Fibrotic Stroma as one of the Main Morphological Components of PDAC	12
2.3. Neuropathic Changes in Pancreatic Cancer and its Clinical Significance	13
2.4. Structure of Pigment Epithelium-Derived Factor (PEDF)	16
2.5. Expression and Biological Functions of PEDF	28
2.6. Aim of the Study	19
3. MATERIALS AND METHODS	20
3.1. MATERIALS	20
3.1.1. Laboratory Equipment	20
3.1.2. Consumables	25
3.1.3. Chemicals	28
3.1.4. Buffers and Solutions	28
3.1.5. Recombinant Human (rH) Protein, siRNA Molecules and ELISA-Kit	22
3.1.6. Antibodies and Negative Controls	25
3.1.7. Biological Materials	30
3.2. METHODS	30
3.2.1. Pancreatic Tissues and Patient Data	30

3.2.2. Pancreatic Cancer Cell Lines	30
3.2.3. Human Primary Pancreatic Stellate Cell (PSC) Isolation and Culture	28
3.2.4. Human Umbilical Vein Endothelial Cell Culture	31
3.2.5. Mouse Neuroblastoma Cell Culture	22
3.2.6. Human Schwann Cell Culture	32
3.2.7. Immortalized Human Pancreatic Duct Epithelial Cell Culture	32
3.2.8. Expression Analyses	32
3.2.8.1. Immunohistochemistry	32
3.2.8.2. Immunofluorescence Analysis	33
3.2.8.3. Immunoblot Analysis	33
3.2.8.4. Real-time Light Cycler® Quantitative Polymerase Chain Reaction	35
3.2.9. PEDF Stimulation of PSCs	37
3.2.10. Induction of Hypoxia	37
3.2.11. siRNA Transfection	38
3.2.12. ELISA	38
3.2.13. 3-(4, 5-methylthiazol-2-yl)-2, 5-diphenyl-tetrazolium-bromide Assay	39
3.2.14. Quantitative Image Analysis	40
3.2.15. Densitometry	40
3.2.16. Statistics	40
4. RESULTS	42
4.1. Assessment of PEDF Expression in Pancreatic Tissues	42
4.2. Localization of PEDF in Pancreatic Tissues	42

4.3. Correlation of PEDF Expression in Cancer Cells and Patient Survival	45
4.4. Correlation of PEDF Expression with Microvessel- and Neural-Densities in Pancreatic Cancer	46
4.5. Expression and Localization of PEDF Receptors in Pancreatic Cancer Tissues and Stellate Cells	50
4.6. Effects of PEDF on Pancreatic Stellate Cell Activity and Extracellular Matrix Protein Production	52
4.7. Regulation of PEDF Expression in Pancreatic Cancer and Immortalized Duct Cell lines by Oxygen	54
4.8. The Effect of Pancreatic Cancer Cell Supernatants with and without PEDF-silencing on Endothelial Cell Growth	57
4.9. The Effect of Pancreatic Cancer Cell Supernatants with and without PEDF-silencing on Nerve Cell Proliferation	59
5. DISCUSSION	61
6. SUMMARY	66
7. REFERENCES	67
8. CURRICULUM VITAE	80
9. ACKNOWLEDGEMENTS	82

## ABBREVIATIONS

$\alpha$ SMA	Alpha smooth muscle actin
Ab	Antibody
APS	Ammonium per sulfate
BSA	Bovine serum albumin
BPE	Bovine Pituitary Extract
CO <sub>2</sub>	Carbon dioxide
CD-31	Cluster of differentiation molecule-31
cDNA	Complementary DNA
COL1	Collagen type 1a
CP	Chronic pancreatitis
°C	Degree Celsius
DAB	3,3'- diaminobenzidine
DAPI	4',6-diamidino-2-phenylindole
DMEM	Dulbecco's modified eagle medium
DMSO	Dimethyl sulphoxide
DNA	Deoxyribonucleic acid
ECL	Enhanced chemoilluminescence
ECM	Extracellular matrix
EGF	Epidermal growth factor
EDTA	Ethylenediamintetraacetic acid
ELISA	Enzyme linked immunosorbent assay
FBN	Fibronectin
FCS	Fetal calf serum
FGF	Fibroblast growth factor
g	Gram
gDNA	Genomic DNA
GAP-43	Growth Associated Protein 43
GAPDH	Glyceraldehyde 3-phospate dehydrogenase
GNDF	Glial cell line-derived neurotrophic factor
h	Hour
HIF 1 $\alpha$	Hypoxia-inducible factor 1 $\alpha$
HPDE	Immortal Human Pancreatic Duct Epithelial cells

HRPO	Horseradish peroxidase
HSC	Human Schwann cells
HUVECs	Human Umbilical Vein Endothelial cells
IB	Immuno-blotting
IL	Interleukin
IgG	Immunoglobulin G
IHC	Immunohistochemistry
kDa	Kilo Dalton
KCl	Potassium chloride
Laminin-R	Laminin receptor
M	Molar
mg	Milligram
ml	Milliliter
µg	Microgram
µl	Microliter
µM	Micromole
mRNA	Messenger ribonucleic acid
MTT	3-(4,5-methylthiazol-2-yl)-2, 5-diphenyl-tetrazolium bromide
MVD	Microvessel density
NaCl	Sodium chloride
nM	Nanomolar
N2a	Mouse neuroblastoma cell-line
OD	Optical density
PanIN	Pancreatic intraepithelial neoplasia
PBS	Phosphate buffered saline
PEDF	Pigment Epithelium-Derived Factor
PDAC	Pancreatic ductal adenocarcinoma
PDGF	Platelet derived growth factor aa
PNPLA2	Patatin-like phospholipase domain-containing protein 2
POSTN	Periostin
PSC	Pancreatic stellate cell(s)
QRT-PCR	Quantitative real-time polymerase chain reaction
RNA	Ribonucleic acid
rPEDF	Recombinant Pigment Epithelium-Derived Factor

RPMI	Roswell Park Memorial Institute (medium)
RT	Room temperature
RtU	Ready to use
SDS	Sodium dodecyl sulfate
siRNA	Small interfering RNA
SFM	Serum-free medium
SM	Standard medium
SN	Supernatant
TBS	Tris-buffered saline
TEMED	Tetramethylethylenediamine
TGF- $\beta$	Transforming growth factor beta
TMB	3,3', 5,5"-tetramethylbenzidine
Tris	Tris(hydroxymethyl)aminomethane
U	Units
V	Volts
VEGF	Vascular endothelial growth factor

## 1. ABSTRACT

**Background:** Pigment Epithelium-Derived Factor (PEDF) is a noninhibitory-member of the serine protease inhibitor gene family with neuroprotective, neuroproliferative, and anti-angiogenic functions. Its role in pancreatic fibrosis and neuropathy is unknown. **Materials and Methods:** The expression and localization of PEDF was assessed by quantitative-RT-PCR, immunohistochemistry, and quantitative image-analysis and correlated with neural- and microvessel-density in the normal pancreas (n=20) and pancreatic cancer (n=55). Primary human pancreatic stellate cells (PSC), mouse neuroblastoma and human Schwann cells were used for functional experiments. The effect of hypoxia on PEDF production in cancer cell lines and immortalized pancreatic ductal epithelial cells was assessed by quantitative-RT-PCR and ELISA. The effect of recombinant PEDF on PSC was assessed by immunoblot analysis. **Results:** PEDF expression was homogenous in the epithelial cells of the normal pancreas where some acinar cells consistently displayed stronger staining. Higher expression was found in tubular complexes, PanIN-lesions and inflammatory cells in pancreatic cancer. Cancer cells expressed various levels of PEDF. In cancer cell lines and in human immortalized pancreatic ductal epithelial cells, hypoxia increased PEDF-mRNA up to 132-fold. Higher expression of PEDF in cancer cells was significantly correlated with better patient survival (median survival 21.5 months vs. 17.5 months,  $p=0.043$ ), increased neuropathy ( $p=0.0251$ ), increased PSC activity and extracellular matrix protein production. **Conclusion:** PEDF increases PSC activity thereby contributing to the desmoplasia of pancreatic cancer. PSC over-activation likely leads to periacinar fibrosis and degeneration of the fine acinar innervation. Increased focal PEDF expression in cancer cells correlates with neuropathic changes and better patient survival.



## 2. INTRODUCTION

### 2.1. PANCREATIC CANCER EPIDEMIOLOGY AND CLINICAL PRESENTATION

Pancreatic cancer is an aggressive and devastating disease, characterized by rapid progression, aggressive invasion of surrounding tissues and early metastasis. The overall median survival time of all patients is around 4-6 months[1]. Pancreatic cancer is the 10<sup>th</sup> most commonly diagnosed cancers with just 3% of all cancers, but it is the 4<sup>th</sup> leading cause of deaths among both men and women, comprising 6% of all cancer-related deaths in western world[2].



FIGURE 1. Ten Leading Cancer Types for Estimated New Cancer Cases and Deaths, by Sex, United States, 2009.  
\*Excludes basal and squamous cell skin cancers and in situ carcinoma except urinary bladder. Estimates are rounded to the nearest 10.

Taken from Cancer Statistics, 2009 (Jemal et al. 2009)[2].

The incidence of the disease has been increasing slowly during the last 10 years[1, 3-4]. The current overall incidence rate of pancreatic cancer is approximately 10 cases per 100.000 persons per year and almost equals its mortality[5]. Unlike other cancers, survival rate of pancreatic cancer has not improved significantly over last 35 years. Since 1975, 5-year survival has increased from 3% to 5%[2]. Pancreatic cancer is extremely difficult to diagnose in its early stages. At the time of diagnosis, 52% of all patients have distant spread and only 7% of patients have localized disease[2].

Although there are several different types of pancreatic cancers, pancreatic ductal adenocarcinoma (PDAC) is the most common form and constitutes more than 85% of all pancreatic malignancies. PDAC is rare in persons younger than 50 years and the risk increases with age. Little is known about the etiology of the disease. Up to 10% of the patients report family history of pancreatic cancer[6]. Smoking[7], diabetes[8], obesity[9], rare familial cancer syndromes[10-13] and chronic pancreatitis[14-16] are substantial risk factors for the development of the disease. Well-known accumulation of genetic and epigenetic changes influences the tumor formation, progression and its aggressive behavior[17-24]. Most commonly mutated gene in PDAC is K-ras seen in 74%-100% of cases[17]. Other involved genes are p16[25], p53[26], DPC4[22] and HER-2/neu[27]. Certain microscopic morphological changes were associated with pancreatic cancer arising from the ductal epithelium of pancreas and pancreatic intraepithelial neoplasia (PanIN) has been identified as the main precursor of PDAC[28-32]. Like pancreatic cancer, prevalence of PanINs increases with age[33] and they are more common in the head of the gland than in the tail[34]. PanINs also share genetic alterations that characterize invasive PDAC[1]. PanIN-3, high-grade PanIN, also referred as 'carcinoma-in-situ'

demonstrates nuclear atypia, loss of polarity and frequent mitosis; however it is still confined to the basement membrane and are present in 30% to 50% of pancreas with invasive ductal carcinoma[35-36].

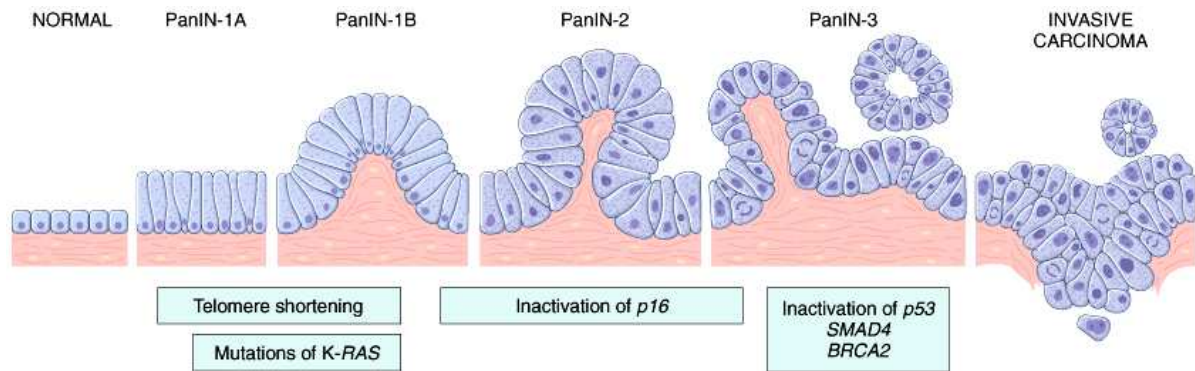


**Figure 19-13** Progression model for the development of pancreatic cancer. It is postulated that telomere-shortening, and mutations of the oncogene *K-RAS* occur at early stages, that inactivation of the *p16* tumor suppressor gene occurs at intermediate stages, and the inactivation of the *p53*, *SMAD4* (*DPC4*), and *BRCA2* tumor suppressor genes occur at late stages. It is important to note that while there is a general temporal sequence of changes, the accumulation of multiple mutations is more important than their occurrence in a specific order. (Adapted from Wilentz RE, Iacobuzio-Donahue CA, et al: Loss of expression of *DPC4* in pancreatic intraepithelial neoplasia: evidence that *DPC4* inactivation occurs late in neoplastic progression. *Cancer Res* 2000; 60:2002.)

Taken from Robbins and Cotran Pathologic Basis of Disease, 7<sup>th</sup> Ed. 2004[37].

The initial symptoms of PDAC are quite nonspecific. Symptoms are primarily caused due to mass effect of the tumor, rather than disruption of pancreatic endocrine and exocrine functions and depend on the size and localization. Most pancreatic carcinomas occur at the head of the pancreas and the characteristic sign is obstructive jaundice. The patients usually notice darkening of urine, lightening of stools, pruritus and changes in skin pigmentation. Weight loss is a characteristic feature of pancreatic cancer and may be due to cancer-related anorexia, or pancreatic insufficiency, resulting in malabsorption and steatorrhea. Another classical symptom is pain. Typically, it is epigastric in location with back radiation and range from dull ache to severe pain. Back pain usually indicates the advanced

disease with retroperitoneal invasion of the nerve plexus by tumor.

Surgical resection is the treatment of choice, but it is only an option in 15%-20% of the patients[38-39]. Even in this case the median survival time is not more than 11 - 18 months[40-42]. Local recurrence with or without distant metastasis develops in 41% and distant metastasis in 49% of patients[43]. Chemotherapy and radiotherapy is offered for the patients who are not surgical candidates, however PDAC has a high resistance to therapy and the treatment often fails[5, 44].

## **2.2. ABUNDANT DENSE FIBROTIC STROMA AS ONE OF THE MAIN MORPHOLOGICAL COMPONENTS OF PDAC**

One of the characteristic histopathologic features of PDAC is replacement of normal pancreatic parenchyma with dense fibrotic stroma surrounding the cancer cells, known as desmoplasia[45]. Fibrosis is the outcome of persistent tissue destruction triggered by mediator-activated transformation of resident fibroblasts to myofibroblasts followed by synthesis and accumulation of extracellular matrix (ECM) components[46-47]. Fibroblasts in pancreatic cancer are now recognized as pancreatic stellate cells (PSCs) - key players in pancreatic fibrogenesis[48-50]. In the normal pancreas PSCs are quiescent, comprise approximately 4% of pancreatic cell population and are identified by the presence of vitamin-A containing droplets in their cytoplasm[50-51]. Release of growth factors and cytokines in response to pancreatic injury results in transformation of PSCs from quiescent into  $\alpha$ -SMA-expressing activated myofibroblasts that proliferate, migrate and synthesize excessive ECM proteins, including collagen type 1, collagen type 3 and fibronectin[50-52]. Potent activators of PSCs are paracrine factors released by inflammatory cells, platelets and cancer cells themselves[48, 53]. Activated PSCs

can also produce autocrine factors (PDGF, TGF $\beta$ <sub>1</sub>, IL-1, IL-6) sustaining their activated phenotype[52, 54-55]. The interactive relationship between cancer cells and stellate cells form complex tumor-stroma structure, which largely affects the overall progression of PDAC[52, 56]. ECM influences growth, survival, differentiation and motility of cancer cells[45]. Cancer cells themselves create tumor supportive microenvironment by production of stroma-modulating growth factors and alteration of adjacent stroma[45, 56].

Pancreatic cancers are hypoxic and hypovascular[57]. Several studies have revealed that hypoxia increases PSCs activity and secretion of PSC-specific ECM protein periostin, as well as collagen type 1 and fibronectin[45, 58-59]. On the other hand, PSCs can be considered as the inducers of tissue hypoxia, due to abnormal production and deposition of ECM proteins[59]. Accumulated stromal proteins can compress blood vessels or form physical barrier interfering the oxygen delivery[59]. Hypoxia and fibrosis commonly occur together and are associated with poor prognosis, resistance to chemotherapy, radiotherapy and increased metastatic potential[60-61].

### **2.3. NEUROPATHIC CHANGES IN PANCREATIC CANCER AND ITS CLINICAL SIGNIFICANCE**

The pancreas has an abundant nerve supply, composed of various myelinated or unmyelinated nerve fibers and aggregates of neural cell bodies known as intrapancreatic ganglia[62]. Innervation of pancreas consists with both, intrinsic and extrinsic neural components. The intrapancreatic ganglia are randomly scattered in the organ parenchyma and comprises intrinsic components of pancreatic nerve supply[62]. An extrinsic component is composed of neurons lying outside the

digestive tract and belongs to sympathetic and parasympathetic autonomic nervous system. The parasympathetic fibers are the branches of vagus nerve and reach the pancreas directly, or passing across the preaortic chain of sympathetic ganglia[62]. The sympathetic fibers are composed of postganglionic fibers, coming from celiac ganglionic plexus, superior mesenteric plexus and hepatic plexus. The autonomic nervous system regulates the secretory functions of pancreas, constriction and relaxation of the blood vessels and excretory ducts[63]. Pancreas has a sensory nerve supply, as well, classified as afferent system involved in signal transmission to the central nervous system[62].

The nerves are usually involved when pathologic changes occur in an organ. In pancreatic cancer involvement of the nerves clinically is demonstrated as a severe abdominal pain, the most distressing symptom of the disease. Pain is reported by 75%-80% of patients at the initial evaluation[64]. The typical pain in locally advanced disease is dull, constant, mid-epigastric in location, with middle or lower back irradiation and may be aggravated by eating or lying flat. Night-time pain often becomes predominant complaint for most of the patients. About one-fifth of patients may not have pain at the time of initial examination, but all the PDAC patients experience pain at some point of the clinical course.

Multiple studies have been conducted to improve understanding the pathophysiology of pain in pancreatic cancer, but the exact mechanism of pain generation remains unclear.

Earlier, the origin of pain in PDAC was considered to be visceral[65-68]. In this case pain is generated by stimulation of pain receptors by infiltration, compression, extension or stretching of abdominal viscera. More recently, there is increased evidence that pain in pancreatic cancer is neuropathic in origin[69]. Neuropathic pain

is caused by injury of peripheral or visceral nerves, rather than stimulation of pain receptors and is a result of nerve compression by tumor, or direct infiltration of nerves by cancer- or inflammatory cells[70]. Once the nerves are damaged, a minimal tissue injury can precipitate the severe pain[70]. Neuropathic pain is a chronic pain state; it is usually severe, deep, aching and is described as electrical, burning or shooting[70]. This type of pain is not self-limited and is not easy to treat[71].

Pancreatic cancer cells are in close contact with intrapancreatic nerves. Perineural invasion is a histopathologic characteristic of PDAC. Infiltration of the intrapancreatic nerves by cancer cells eventually leads to the extrapancreatic nerve plexus invasion, leading to retropancreatic cancer extension, precluding curative resection and promoting local recurrence after tumor resection[72].

Intrapancreatic nerves in PDAC undergo neuropathic morphologic alterations, demonstrated as pathologic enlargement of the nerve fibers, leading to the pain[73]. Nerves in chronic pancreatitis (CP) and PDAC are characterized by neural plasticity[73]. Both diseases create a special intrapancreatic microenvironment by inflammation and secretion of certain neurotrophic factors. This intrapancreatic microenvironment stimulates the nerves to undergo neuroplastic changes leading to the enlargement of a single nerve fiber[74]. The analysis of pancreatic nerves in tissues removed from the patients with chronic pancreatitis revealed that the mean diameter of nerves in the patients with CP was significantly greater in comparison to controls[75]. These neuropathic changes are typical feature of PDAC and CP and was not detected in other disorders of pancreas[76].

## **2.4. STRUCTURE OF PIGMENT EPITHELIUM-DERIVED FACTOR**

Pigment Epithelium-Derived Factor (PEDF) is a 50-kDa glycoprotein and noninhibitory member of the serine protease inhibitor gene family[77-78]. The gene encoding the human PEDF is localized to chromosome 17p13.3, spans approximately 16kb and contains eight small exons and seven introns, with the largest intron 4kb in length[79]. The transcription factors regulating PEDF expression are not yet identified[79]. PEDF is expressed continuously in different cell types. Its expression is modified during diseases and regulated by senescence of the cells[79]. PEDF shares sequence homology with the other members of serpin superfamily of serine protease inhibitors, but lacks sequence for the serpin reactive center region and does not demonstrate antiprotease activity[77]. The gene contains an open reading frame encoding a 418 amino-acid protein[79]. N-terminal portion, residues 1-19, contains a leader sequence responsible for protein secretion from the cell[80]. Near the C-terminal portion, residues 365-390, forms the reactive center loop of protein[78].

Generation of the crystal structure of PEDF allowed 3-D structural analysis of the protein[79, 81]. With exception of 15 residues at the N-terminal and 8 residues in the reactive center loop, all the molecule backbone is well ordered[81]. N- and C-termini of the reactive center loop are well defined, but central 8 residues have no electron density[81]. PEDF structure includes 3 beta sheets and 10 alpha helices, what reveals the very asymmetric charge distribution across the whole protein[81]. Highly acidic region is located around the N-terminal part of the molecule at the opposite side from the highly basic region[81]. Different regions of the molecule are involved in the various biological activities of PEDF[82]. 34-mer fragments (residues 24-57)



produce angioinhibitory signals, whereas 44-mer fragment with residues 58-101 is responsible for the neurotrophic properties of PEDF [82].

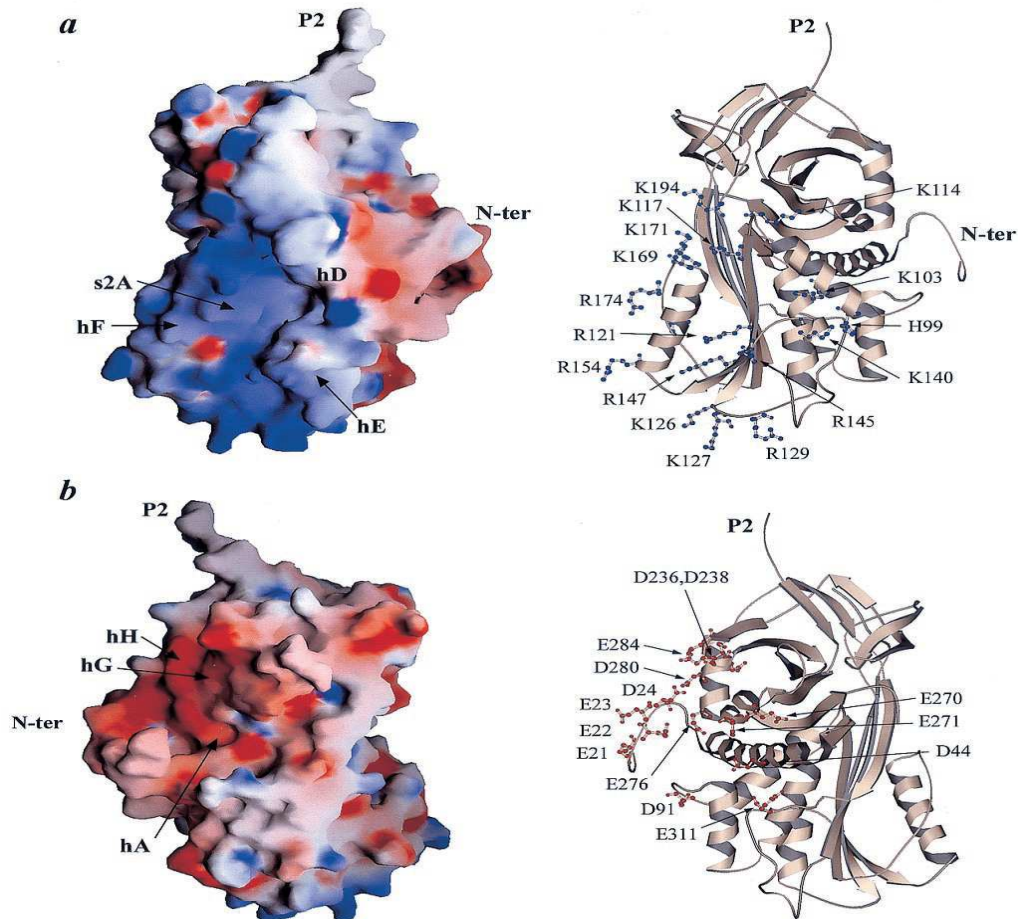


**Fig. 3.** Surface charge distribution analysis of PEDF reveals striking asymmetric charge distribution that might be of physiological significance. (*Left*) GRASP (35) representations are displayed. (*Right*) Ribbon diagrams of PEDF oriented in the same way as the respective surface charge diagrams, with basic (blue) and acidic (red) side chains presented as ball-and-stick (scale, 215 kTye to 115 kTye). (*a*) The basic region that covers parts of hD, hE, s1A, and s2A is displayed. This is the putative heparin-binding site. The view is rotated 90° clockwise about the vertical axis relative to Fig. 1. (*b*) The acidic region consists of side chains from the extreme N terminus, hA, s6B, hG, and hH. The view is rotated 90° counterclockwise about the vertical axis relative to Fig. 1.

*Taken from Crystal structure of human PEDF, a potent anti-angiogenic and neurite growth-promoting factor. (Simonovic et al. 2001)[81].*

## 2.5. EXPRESSION AND BIOLOGICAL FUNCTIONS OF PEDF

PEDF was originally isolated from conditioned medium of cultured human fetal retinal pigment epithelium cells, inducing neuronal differentiation in human Y-79

retinoblastoma cells in vitro[83-85]. PEDF is found in almost all tissues with the highest expression being observed in the fetal and adult liver, adult testis, ovaries, placenta and the pancreas[86]. Its expression is significantly reduced in senescent cells[79, 87-89]. The most studied attributes of PEDF are its neuroprotective, neuroproliferative, and anti-angiogenic functions. As observed in the retina, PEDF strongly stimulates the growth of neural derived cells while it actively suppresses endothelial growth. Beyond its function in the retina, PEDF is known to exert neurotrophic properties in several other neural cells, such as Y79 cells[83-84], cerebellar granule cells[90], glial cells[91] and motor neurons[92-93].

In contrast, PEDF inhibits endothelial cell growth and neovascularization by induction of apoptosis, whereas the existing vasculature remains intact[94]. PEDF is more potent than any other known inhibitor of angiogenesis such as endostatin, angiostatin and thrombospondin-1[94]. PEDF can also block angiogenic effects of VEGF, FGF and IL-8[94]. At the protein level, the amount of PEDF produced positively correlates with oxygen concentration[94].

PEDF knock-out mice exhibit not only retinal and nervous system abnormalities but also strong hypervascularization and epithelial hyperplasia in the pancreas and prostate[95]. In humans, PEDF expression in pancreatic ductal adenocarcinoma cells (PDAC) positively correlates with a favorable survival and negatively correlates with the presence of liver metastasis[96]. Similarly, PEDF over-expressing pancreatic tumors in mice were smaller than the controls and intratumoral injection of lentivirus vector encoding PEDF caused a significant inhibition of tumor growth[97].

## **2.6. AIM OF THE STUDY**

In this study, we evaluated the effects of PEDF expression of cancer cells on intrapancreatic neuropathy, pancreatic stellate cell activity and fibrosis. Our results show that while the nerve caliber in the diseased pancreas increases, there is a significant loss of the fine innervation seen in the periacinar spaces accompanying the periacinar fibrosis. Since this distortion of normal pancreatic architecture is accompanied by stromal activation in the periacinar spaces, we also analyzed the effects of PEDF on pancreatic stellate cells in terms of activity and fibrogenesis.

### 3. MATERIALS AND METHODS

#### 3.1. MATERIALS

##### 3.1.1. Laboratory Equipment

Analytic balance	Mettler-Toledo, Inc. Columbus, USA
Balance	Scaltec Instruments, GmbH. Göttingen, Germany
Bio-Photometer	Eppendorf AG, Hamburg, Germany
Cell culture hood	Thermo Fisher Scientific Inc. Langenselbold, Germany
Centrifuges:	
Heraeus Multifuge 3SR	Thermo Fisher Scientific Inc. Langenselbold, Germany
Centrifuge 5415R	Eppendorf AG, Hamburg, Germany
CO <sub>2</sub> Incubator	Thermo Fisher Scientific Inc. Langenselbold, Germany
Computer Hardware	Fujitsu SIEMENS, München, Germany
DNA/RNA UV Cleaner Box	Lab4You, Berlin, Germany
Electrophoresis/Electroblotting systems	Invitrogen, Karlsruhe, Germany
Embedding machine	Leica, Bensheim, Germany
Freezer -20°C	Liebherr, Ochsenhausen, Germany
Freezer -80 °C	Thermo Fisher Scientific Inc. Langenselbold, Germany
Hypoxia chamber	Billups-Rothenberg inc. Del Mar, CA, USA
Ice machine	Scotsman, Milan, Italy

Liquid nitrogen tank	Taylor-Wharton, Husum, Germany
Magnetic stirrer: Ika-Combimag RET	Jahnke & Kunkel , Staufen i. B., Germany
Microplate ELISA-reader	Thermo Electron GmbH, Karlsruhe, Germany
Microscopes:	
Inverted Microscope	Carl Zeiss, Jena, Germany
Light Microscope	Carl Zeiss, Jena, Germany
Microtome	Leica, Bensheim, Germany
Microwave oven	Siemens, München, Germany
NanoPhotometer	Implen, München, Germany
PH-meter	WTW GmbH, Weilheim, Germany
Power-Supply	Biometra, Goettingen, Germany
QT-PCR: LightCycler Instrument	Roche, Mannheim, Germany
Refrigerator 4 °C	Liebherr, Ochsenhausen, Germany
Roller mixer	Progen Scientific, London, UK
Scanner	Canon, Tokyo, Japan
Thermomixer	Eppendorf, Wesseling, Berzdorf, Germany
Tissue embedding machine	Leica, Bensheim, Germany
Tissue processor	Leica, Bensheim, Germany
Vortex	IKA Works, Inc. Wilmington, NY
Water bath 37°C	Lauda-Königshofen, Lauda, Germany
Water Distillator	Millipre, Schwallbach, Germany
X-ray film cassette	Eastman Kodak Company, Rochester, NY, USA

### 3.1.2. Consumables

Cell culture dishes 35-3003 20mm	BD Bioscience, Heidelberg, Germany
Cell culture dishes 75cm <sup>3</sup>	BD Bioscience, Heidelberg, Germany
6-well plates	BD Bioscience, Heidelberg, Germany
24-well plates	BD Bioscience, Heidelberg, Germany
96-well plates	BD Bioscience, Heidelberg, Germany
Cell Scraper BD®	Bioscience, Heidelberg, Germany
Cotton swabs	NOBA, Wetter, Germany
Cover slips	Marienfeld, Lauda-Königshofen, Germany
Disposable Scalpel	Feather, Fukushima, Japan
Eppendorf® 1,5ml Tubes	Eppendorf AG, Hamburg, Germany
Falcon® Röhrchen 15ml pp-test tubes	BD Bioscience, Heidelberg, Germany
Falcon® Röhrchen 50ml pp-test tubes	BD Bioscience, Heidelberg, Germany
Gel blotting Paper	Whatman, Sanford, ME, USA
Glass slides	Menzel, Braunschweig, Germany
Negative film, Hyperfilm®	Amersham, Buckinghamshire, UK
Nitrocellulose-transfer membrane	Bio-Rad, Hercules, CA, USA
Parafilm	Pechiney plastic packaging, Chicago, USA
Sterile needle	BD Bioscience, Heidelberg, Germany
Pipet tips	Biozym, Oldendorf, Germany
Teflon-coated slides	Erie Scientific Co, Portsmouth, NH

### 3.1.3. Chemicals

0.25% trypsin/EDTA	Invitrogen GmbH, Karlsruhe, Germany
10% Tris-HCl gels	Bio-Rad, Hercules, CA, USA

2-Mercaptoethanol	Sigma-Aldrich, Taufkirchen, Germany
3-(4,5-methylthiazol-2-yl)-2,5-diphenyltetrazolium bromide	Sigma-Aldrich, Taufkirchen, Germany
Acetic acid	Merck Biosciences, Schwalbach, Germany
Acrylamide/Bis solution	Bio-Rad, Hercules, CA, USA
Agarose	Invitrogen GmbH, Karlsruhe, Germany
Ammonium per sulfate (APS)	Sigma-Aldrich, Taufkirchen, Germany
Amphotericin-B	PAA, Pasching, Austria
B-27 serum-free supplement	Invitrogen GmbH, Karlsruhe, Germany
Bovine Pituitary Extract (BPE)	Invitrogen GmbH, Karlsruhe, Germany
BCA Protein Assay Kit	Thermo Scientific, Rockford, Illinois, USA
Bovine Serum Albumin	Roth, Karlsruhe, Germany
Bromophenol blue	Sigma-Aldrich, Taufkirchen, Germany
DetachKit	Promocell, Heidelberg, Germany
Dimethylsulfoxid	Sigma-Aldrich, Taufkirchen, Germany
DMEM	Invitrogen GmbH, Karlsruhe, Germany
ECL® detection reagent	Amersham Biosciences, Freiburg, Germany
Endothelial cell growth medium	Promocell, Heidelberg, Germany
Envision antibody diluent	Dako GmbH, Hamburg, Germany
Epidermal Growth Factor (EGF)	Invitrogen GmbH, Karlsruhe, Germany
Ethanol	Roth, Karlsruhe, Germany
Ethidium bromid	Sigma-Aldrich, Taufkirchen, Germany
Fetal Calf Serum	PAN Biotech, Aidenbach, Germany
Glycerol	Merck Biosciences, Schwalbach, Germany
Glycin	Roche diagnostics, Mannheim, Germany

Haematoxylin	Merck Biosciences, Schwalbach, Germany
HiPerFect transfection reagent	Qiagen, Hilden, Germany
Hydrogen peroxide	Roth, Karlsruhe, Germany
Ham's F12 medium	Invitrogen GmbH, Karlsruhe, Germany
Histowax	Leica, Bensheim, Germany
Humidified chamber	TeleChem International Inc., USA
Hydrogen peroxide	Roth, Karlsruhe, Germany
Isopropanol	Roth, Karlsruhe, Germany
Keratinocyte-SFM	Invitrogen GmbH, Karlsruhe, Germany
Laurylsulfat (SDS)	Roth, Karlsruhe, Germany
LightCycler 480 DNA SYBR Green I	
Master kit	Roche diagnostics, Mannheim, Germany
Liquid nitrogen	TMG Sol Group, Gersthofen, Germany
Liquid DAB & chromogen substrate	Dako GmbH, Hamburg, Germany
Methanol	Roth, Karlsruhe, Germany
Molecular weight marker	Fermentas, Life Sciences, Ontario, Canada
NaCl	Fluka Chemie, Buchs, Switzerland
Neurobasal medium	Invitrogen GmbH, Karlsruhe, Germany
Nitrocellulose membranes	Bio-Rad, Hercules, CA, USA
Paraformaldehyde	Fischer, Kehl, Germany
PBS pH 7.4	Invitrogen GmbH, Karlsruhe, Germany
PCR amplification kit	Roche diagnostics, Mannheim, Germany
Penicillin-Streptomycin	Invitrogen GmbH, Karlsruhe, Germany
Potassium chloride (KCl)	Merck Biosciences, Schwalbach, Germany
Premount® – Mounting Medium	Fischer, Kehl, Germany



Proteinase K	Sigma-Aldrich, Taufkirchen, Germany
Proteaseinhibitor Cocktail	Roche diagnostics, Mannheim, Germany
QuantiTect Rev. Transcription Kit	Qiagen, Hilden, Germany
RNAse-DNAse-free water	Invitrogen GmbH, Karlsruhe, Germany
RPMI 1640 Medium	Invitrogen GmbH, Karlsruhe, Germany
Roticlear®	Roth, Karlsruhe, Germany
RNeasy Mini Kit	Qiagen, Hilden, Germany
Sodium borate	Merck Biosciences, Schwalbach, Germany
Sodium chloride	Merck Biosciences, Schwalbach, Germany
Sodium citrate	Merck Biosciences, Schwalbach, Germany
Sodium phosphate	Merck Biosciences, Schwalbach, Germany
SupplementMix	Promocell, Heidelberg, Germany
TEMED	Sigma-Aldrich, Taufkirchen, Germany
Toluidin blue	Merck Biosciences, Schwalbach, Germany
Tris Base	Merck Biosciences, Schwalbach, Germany
Triton-X-100	Merck Biosciences, Schwalbach, Germany
Trypan blue solution	Sigma-Aldrich, Taufkirchen, Germany
Tween 20	Merck Biosciences, Schwalbach, Germany

### 3.1.4. Buffers and Solutions

Immunohistochemistry:

10 X Tris buffered saline (TBS)

Tris base	12.1 g
NaCl	85 g
H <sub>2</sub> O	800 ml

pH to 7.4 with 5M HCl  
add H<sub>2</sub>O to 1000 ml

#### 1 X TBS/0.1% BSA

10XTBS 100ml  
BSA 1 g  
add H<sub>2</sub>O to 1000 ml

#### 1 X TBS/0.1% BSA/0.05% Tween 20

1XTBS/0.1% BSA 1000ml  
Tween 20 500 µl

#### 1 X TBS/3% BSA

1XTBS 100ml  
BSA 3 g

#### Peroxidase Block

Methanol 900 µl  
Wasserstoff Peroxid 100 µl

#### Protein Extraction and Immunoblotting:

##### Lysis Buffer

1M Tris-HCl(pH=7.5) 0.5ml  
5M NaCl 0.3ml  
0.5M EDTA(pH=8) 40 µl

20% SDS	500 µl
add H <sub>2</sub> O to	9 ml
Proteinase Inhibitor	1 tablet

#### Sample Buffer

1.25M Tris-HCl	100 µl
10% SDS	50 µl
87% Glycerol	95 µl
Mercaptoethanol	25 µl
Bromphenolblue	5 µl

#### Electrophoresis Buffer

Tris	30.25g
Glycin	144g
1%SDS	50ml
add H <sub>2</sub> O to	1000 ml

#### Blotting Buffer

Tris	3.03g
Glycin	14.4g
10%SDS	3ml
add H <sub>2</sub> O to	800 ml
Methanol	200 ml

## Stripping Buffer

Glycin	15g
add H <sub>2</sub> O to	1000 ml
pH to 2.5 with	5M HCl

### 3.1.5. Recombinant Human (rH) Protein, siRNA Molecules and ELISA-Kit

Recombinant Human PEDF (P232)	Leinco Technologies, Inc. St. Louis, MI
PEDF small interfering RNA (siRNA) (am16708)	Ambion, Huntingdon, UK
Negative control siRNA (4390843)	Ambion, Huntingdon, UK
PEDF ELISA (PED613) kit	Bioproducts, Middletown, MD

### 3.1.6. Antibodies and Negative Controls

Alexa Fluor 488 goat anti-rabbit IgG (A-11008)	Invitrogen GmbH, Karlsruhe, Germany
Alexa Fluor 680 donkey anti-sheep IgG (A-21102)	Invitrogen GmbH, Karlsruhe, Germany
Anti-collagen type-1 (sc-8783)	Santa Cruz Biotechnology Santa Cruz, CA, USA
Anti-GAP43 Ab. (MAB347)	Chemicon, Temecula, CA
Anti GAPDH Ab. (sc25778)	Santa Cruz Biotechnology Santa Cruz, CA, USA
Anti-goat secondary Ab. (sc-2056)	Santa Cruz Biotechnology Santa Cruz, CA, USA

Anti-Hif 1 alpha Ab. (sc-10790)	Santa Cruz Biotechnology Santa Cruz, CA, USA
Anti-human CD31 Ab. (M0823)	Dako GmbH, Hamburg, Germany
Anti-human fibronectin (F3648)	Sigma-Aldrich Taufkirchen, Germany
Anti-human PEDF Ab. (sc-25594)	Santa Cruz Biotechnology Santa Cruz, CA, USA
Anti-human smooth muscle actin (SMA) (M0851)	Dako GmbH, Hamburg, Germany
anti-Laminin-R Ab. (sc-20979)	Santa Cruz Biotechnology Santa Cruz, CA, USA
Anti-mouse secondary Ab. (NA931V)	Amersham Biosciences, Buckinghamshire,UK
Anti-rabbit secondary Ab. (NA934V)	Amersham Biosciences, Buckinghamshire,UK
anti-PEDF-R Ab. (AF5365)	R&D systems, Inc. Minneapolis, USA
Anti-POSTN (RD181045050)	Biovendor, Heidelberg, Germany
HRP Labelled Polymer Anti-Mouse (K4001)	Dako GmbH, Hamburg, Germany
HRP Labelled Polymer Anti-Rabbit (K4003)	Dako GmbH, Hamburg, Germany
IgG1 negative controls (mouse & rabbit)	Dako GmbH, Hamburg, Germany
Rabbit anti-Sheep IgG (61-8620)	Invitrogen GmbH, Karlsruhe, Germany

### **3.1.7. Biological Material**

Collection and usage of biologic materials are described in the appropriate methods sections.

## **3.2. METHODS**

### **3.2.1. Pancreatic Tissues and Patient Data**

Data on patient survival, tumor stage (UICC 2002) and applied treatments were analyzed retrospectively from a prospectively registered data base. Tissue samples were collected from patients following pancreatic resection for PDAC at the University of Bern, Switzerland, and the University of Heidelberg, Germany. All patients were informed and written consent was obtained. The studies were approved by the Ethics Committees of the University of Bern and the University of Heidelberg. Normal pancreatic tissue samples were obtained at the University of Bern through an organ donor procurement program whenever there was no suitable recipient for pancreas transplantation. All samples were confirmed histologically. Freshly removed tissues were fixed in 4% paraformaldehyde solution for 12 to 24 hours and then paraffin embedded for histological analysis. In addition, a portion of the tissue samples were either snap frozen in liquid nitrogen immediately upon surgical removal and stored at  $-80^{\circ}$  C for protein extraction or preserved in RNA-later (Ambion Europe Ltd., Huntingdon, Ambridgeshire, UK) for future RNA extraction.

### **3.2.2. Pancreatic Cancer Cell Lines**

Pancreatic cancer cell lines Aspc-1, Bxpc-3, Capan-1, Colo-357, Miapaca-2, Panc-1, SU86.86, and T3M4 were used. Cells were either purchased from ATCC (Rockville,

MD, USA) or received as a kind gift of Dr. R. S. Metzgar (Durham, NC, USA). The cells were routinely grown in complete medium (RPMI 1640 supplemented with 10% FCS, 100 U/mL penicillin, and 100µg/mL streptomycin) at 37°C in a humid chamber, saturated with 5% CO<sub>2</sub>.

### **3.2.3. Human Primary Stellate Cell Isolation and Culture**

Human PSC isolation and culture were performed as described by Bachem et al.[51] according to the following protocol: Pancreatic tissue was obtained during surgery from patients with PDAC. For the isolation of PSC, histologically fibrotic areas of the pancreas were utilized for outgrowth. Small tissue blocks were cut (0.5-1mm<sup>3</sup>) using a razor blade and were seeded in 10cm<sup>2</sup> uncoated Petri dishes in the presence of 20% FCS in a 1:1 (vol/vol) mixture of Dulbecco's modified Eagle medium with Ham's F12 medium, penicillin 1%, streptomycin 1% and amphotericin 1% (SM-20%). Tissue blocks were cultured at 37°C in a 5% CO<sub>2</sub>-air humidified atmosphere. After reaching confluency, cells were subcultured by trypsinization. Passage-2 is a 1:2 division of these cells into two new T75 cm<sup>2</sup> flasks. When passage-2 cells reached confluency, they were aliquoted and frozen. For experiments, aliquots of PSCs were thawed in SM and grown to 70% confluency in 75 cm<sup>2</sup> culture flasks (accepted as passage 2). Cell populations between passage 3 and 6 were used for experiments.

### **3.2.4. Human Umbilical Vein Endothelial Cell Culture**

Human Umbilical Vein Endothelial cells (HUVECs) were purchased from Promocell (Heidelberg, Germany) and cultivated in endothelial cell growth medium supplemented with SupplementMix, at 37°C in a humid chamber, saturated with 5% CO<sub>2</sub>.

### **3.2.5. Mouse Neuroblastoma Cell Culture**

Mouse neuroblastoma cells (N2a) were received as a kind gift of Prof. Karl-Herbert Schäfer (Zweibrücken, Germany). The cells were grown in Dulbecco's modified Eagle's medium supplemented with penicillin, streptomycin, and 10% FCS, at 37°C in a humid chamber, saturated with 5% CO<sub>2</sub>.

### **3.2.6. Human Schwann Cell Culture**

Human Schwann cells (HSCs) were purchased from ScienCell Research Laboratories (Carlsbad, CA) and cultivated in Neurobasal medium in combination with B-27 serum-free supplement, at 37°C in a humid chamber, saturated with 5% CO<sub>2</sub>.

### **3.2.7. Immortalized Human Pancreatic Duct Epithelial Cell Culture**

Immortalized Human Pancreatic Duct Epithelial cells (HPDE) were a kind gift from Prof. M.S. Tsao from Ontario Cancer Institute (Toronto, Canada). The cells were grown in Keratinocyte-SFM supplemented with Epidermal Growth Factor (EGF), Bovine Pituitary Extract (BPE) and antibiotics, at 37°C in a humid chamber, saturated with 5% CO<sub>2</sub>. The medium was replaced every two to three days.

### **3.2.8. Expression Analyses**

#### **3.2.8.1. Immunohistochemistry**

Two sequential 3 µm thick formalin fixed, paraffin-embedded tissue sections were placed on the same slide, de-paraffinized and re-hydrated gradually. One section was used for analysis while the other was used as the negative control. Antigen retrieval was performed by boiling the slides in 10 mM citrate buffer two times for 10



min. Peroxidase activity was quenched with a 3% H<sub>2</sub>O<sub>2</sub> solution in 30% methanol. DakoCytomation antibody diluent was used to dilute both the primary antibody and the appropriate negative-control. After an overnight incubation at 4°C, slides were washed with Tris buffer supplemented with 0.05% Tween-20 (TBS-T) for 2 times, and exposed to the HRPO-linked secondary antibody for 60 min at room temperature. Color reaction was carried out by incubation for 1 min with liquid DAB+substrate and counter-staining by Mayer's hematoxylin solution and mounted. Staining with CD31 and GAP43 was carried out without counterstaining to yield better quantification of microvessel- and nerve-densities, respectively. A Zeiss Axiocam ICc 3 system was used for microphotography. Antibody dilutions are shown in Table 1.

### **3.2.8.2. Immunofluorescence Analysis**

PSCs were seeded on Teflon-coated slides at a density of 5000/well in 100µl SM 10%. Twenty-four hours later, cells were fixed with 4% paraformaldehyde, permeabilized with 0.1% Triton X-100, and incubated with primary antibodies overnight at 4°C. The secondary antibodies and 4',6-diamidino-2-phenylindole (DAPI) were used appropriately. Antibody dilutions are shown in [Table 1](#).

### **3.2.8.3. Immunoblot Analysis**

For the immunoblot analyses, cells were grown on 6-WPs. Cells were washed twice with ice-cold PBS. Cell culture monolayers were homogenized and lysed with 0.1 ml buffer containing Tris-HCl (pH: 7.5), 150 mM NaCl, 2 mM EDTA, 1% SDS, and one tablet of complete mini-EDTA-free protease inhibitor cocktail (per 10 ml of the buffer). The cells were scraped off from the dish. The cell extracts were

homogenized by passing through a syringe G27 needle 10 times. The crude homogenate was then centrifuged at 14,000 g in a precooled centrifuge for 15 minutes. The supernatant was immediately transferred to fresh tubes and aliquoted. The sample aliquots were stored at -20<sup>0</sup>C or used for Western blotting analysis immediately. Protein concentration was determined by BCA protein assay. The cell extract (5 µl) was diluted in 100µl of BCA reagent mixture according to the manufacturer's instructions, and incubated at 37°C for 30 min. The OD was measured with the ELISA reader at 570 nm and calculated with reference to a BSA standard curve (0-2 mg/ml). Samples containing 20 µg of the protein extract were size-fractionated by 10% SDS-PAGE and transferred onto nitrocellulose membranes by the application of 30 V for 75 minutes. Blots were blocked with 20ml TBS-T plus 5% non-fat milk for 20 min., incubated with the primary antibodies overnight at 4<sup>0</sup> C, washed with TBS-T, and incubated with the appropriate secondary antibodies for two hour at room temperature. After washing with TBS-T, antibody detection was performed using the enhanced chemoilluminescence (ECL) reaction system. Each membrane was stripped and reblotted consecutively with GAPDH to verify equal loading. To detect secreted proteins in the supernatants (SN), cells were grown until 100% confluency in 6-WPs and thereafter kept in serum free SM for 24 hours. After collection of the supernatant, cells were counted by trypan blue to exclude the effect of increased cell number ( $\pm 10\%$ ) on the protein level of SN. Fifteen µg protein were size fractionated in the presence of sample buffer without boiling. Antibodies were diluted as specified in Table 1.

**IMMUNOHISTOCHEMISTRY    IMMUNOFLUORESCENCE    IMMUNOBLOTTING**

ANTIBODY	PRIMARY	SECONDARY	PRIMARY	SECONDARY	PRIMARY	SECONDARY
PEDF	1:1000	RtU	---	---	---	---
CD31	1:50	RtU	---	---	---	---
GAP-43	1:4000	RtU	---	---	---	---
Laminin-R	1:100	RtU	1:100	1:200	---	---
PNPLA2	1:25	1:1000	1:25	1:200	---	---
POSTN	1:4000	RtU	---	---	1:3000	1:3000
COL1	---	---	---	---	1:1000	1:2500
Fibronectin	1:1500	RtU	---	---	1:15000	1:10000
$\alpha$ -SMA	---	---	---	---	1:10000	1:5000
HIF 1 $\alpha$	---	---	---	---	1:1000	1:2000
GAPDH	---	---	---	---	1:10000	1:10000

**Table 1.** Antibody Dilutions for Immunohistochemistry, Immunofluorescence and Immunoblotting Analyses. RtU: ready to use.

### 3.2.8.4. Real-time Light Cycler® Quantitative Polymerase Chain Reaction

Total cellular RNA isolation and RNA extraction from normal and PDAC tissues and from the pancreatic cancer and Immortalized Human Pancreatic Duct Epithelial cells was performed using the RNeasy Mini Kit according to the manufacturer's instructions: The frozen tissue was homogenized and disrupted using 600 $\mu$ l RLT buffer. The lysate was passed at least 5 times through a blunt 20-gauge needle fitted to an RNase-free syringe and centrifuged for 3 minutes at full speed. The supernatant was removed and transferred into a new microcentrifuge tube. Cells were grown as monolayers on 6-WPs. After complete aspiration of the medium, 350 $\mu$ l RLT buffer was added to the cell-culture dish. The lysates were collected with a rubber policeman. Then each lysate was placed into a microcentrifuge tubes,

mixed well to ensure that no cell clumps are visible and were passed through a blunt gauge needle fitted to the RNase-free syringe at least 5 times. The following steps were common for RNA isolation from the tissues and from the cells: 1 volume of 70% ethanol was added to the homogenized lysates, and mixed well by pipetting, without centrifuging. 700  $\mu$ l of the sample, including any precipitate that may have formed, was transferred to an RNeasy spin column placed in a 2 ml collection tube and was centrifuged for 15 seconds at  $\geq 8000\times g$ . The flow-through was discarded. 700  $\mu$ l of RW1 Buffer was added to the RNeasy spin column and centrifuged for 15 seconds at  $\geq 8000\times g$  again. The flow-through was discarded. Then, 500  $\mu$ l of RPE Buffer was added to the RNeasy spin column, centrifuged again for 15 seconds and flow-through was discarded. After, 500  $\mu$ l of RPE Buffer was added and the columns were centrifuged for 2 min at  $\geq 8000\times g$  to wash the spin column membrane. The flow-through was discarded. Next, the RNeasy spin columns were placed into a new 2 ml collection tubes and centrifuged at full speed for 1 min. The RNeasy spin columns were placed into a new 1.5 ml collection tube, 30-50  $\mu$ l RNase-free water was added directly to the spin column membrane and centrifuged for 1 min at  $\geq 8000\times g$  to elude the RNA. This step was repeated using the elute that formed before. The isolated RNA was stored at  $-80^{\circ}\text{C}$ .

cDNA was synthesized from total RNA by reverse transcription using the QuantiTect Reverse transcription kit according to the following protocol: The concentration of RNA was measured by NanoPhotometer. The genomic DNA elimination reaction components were prepared with gDNA Wipeout Buffer 2  $\mu$ l, variable amount of template RNA and RNase-free water and incubated for 2 minutes at  $42^{\circ}\text{C}$ . Immediately after incubation the tubes were placed on ice. Next, the reverse-transcription master mix was prepared with Quantiscript Reverse Transcriptase 1  $\mu$ l,

Quantiscript RT Buffer 4  $\mu$ l, RT Primer Mix 1  $\mu$ l and entire genomic DNA elimination reaction product 14  $\mu$ l (from the former step). The mixed components were incubated first for 15 minutes at 42°C and then for 3 min at 95°C to inactivate Quantiscript Reverse Transcriptase. Prepared cDNA samples were stored at -20°C. Real-Time PCR was performed with the LightCycler 480 DNA SYBR Green I Master kit. The samples were prepared with SYBR Green master mix 10  $\mu$ l, primer mix 2  $\mu$ l, PCR-Grade water 3  $\mu$ l and cDNA 5  $\mu$ l.

The primer sets were designed for PEDF (forward 5'-TCT CAA ACT TCG GCT ATG ACC TGT-3', reverse 5'-AGA GCC CGG TGA ATG ATG GAT TCT-3'). The target concentration was expressed as a ratio relative to the expression of the reference gene ( $\beta$ -actin) in the same sample and normalized to the calibrator sample.

### **3.2.9. PEDF Stimulation of PSCs**

Sister clones of PSCs were grown in 6-well plates to 80% confluence. Cells were starved with serum-free medium (SFM) for 24h. Fresh SFM containing 0, 2 or 4 nM recombinant human PEDF was added to the cells. After 72h cell lysates and matching supernatants were collected. All experiments were repeated three times.

### **3.2.10. Induction of Hypoxia**

Pancreatic cancer and HPDE cells were incubated in the modular chamber under a hypoxic gas mixture (89.25% N<sub>2</sub>, 10% CO<sub>2</sub>, 0.75%O<sub>2</sub>) for 12, 16 and 48h at 37°C. The sister clones of the hypoxic cells were incubated under normoxic conditions for the same time periods, at 37°C in a humid chamber, saturated with 5% CO<sub>2</sub>. All experiments were repeated three times.

### **3.2.11. siRNA Transfection**

MiaPaCa-2 and Panc1 cells were seeded in 6-well plates in duplicates at the density of  $2.5 \times 10^5$  cells/well in 2.5 ml of complete medium. Twenty-four hours later, when the cells reached 70% confluence, the old medium was replaced with 2.3ml RPMI1640, containing 10% FCS. Next, the cells were transfected with 10 nM specific PEDF siRNA or negative control siRNA. The following solutions were mixed and kept at RT for 10 minutes, before adding onto cells: 1.2 $\mu$ l PEDF siRNA (10nM), or the same volume of the negative control siRNA + 24 $\mu$ l HiPerFect transfection reagent + 74.8  $\mu$ l SM-0%. After the 10 minutes the mixture was added drop-wise onto the cells.

For mRNA analysis cells were harvested at 24h. For ELISA, the medium was changed to SFM at 48 hours after transfection and at 96 hours the supernatants was collected. All experiments were repeated three times.

### **3.2.12. ELISA**

Twenty four hour supernatants from normoxic and hypoxic pancreatic cancer and HPDE cell lines and 96h supernatants from siRNA transfected cancer cells were collected, centrifuged immediately, aliquoted, frozen and stored at -80°C until use. For quantification of PEDF, a commercially available ELISA kit was used according to the manufacturer's instructions. Briefly, the microwells were pre-coated with a polyclonal antibody specific for full-length recombinant human PEDF antigen. Just before starting the experiment, the PEDF antigen standards were lyophilized in 1,5ml Eppendorf tubes, by adding 500 $\mu$ l of Assay Diluent. A series of six standards was prepared, by further dilution of the PEDF antigen standard stock solution. Next, the microwells were washed 5 times with 200 $\mu$ l of 1X Wash Buffer. 100 $\mu$ l of PEDF

antigen standards and the cell culture supernatants were added to the microplate wells and incubated for 1 hour at 37°C. The samples were aspirated; the wells were washed 5 times with 200µl of 1X Wash Buffer and 100µl of reconstituted PEDF Detector Antibody was added to the each well. The microplate was incubated for 1 hour at 37°C. The samples were aspirated again; the wells were washed 5 times with 200µl of 1X Wash Buffer and 100µl of Streptavidin Peroxidase Working Solution was added to the each well. The microplate was incubated for 30 minutes at 37°C. Next, the samples were aspirated; the wells were washed, 100µl of pre-warmed to room temperature TMB Substrate was added to each well and incubated for 20 minutes at room temperature. A blue color develops in wells containing PEDF antigen. Colorimetric reaction was stopped by adding 100µl of stop solution into each well. The color changes from blue to yellow. The optical density was measured at 450 nm using a Microplate ELISA-reader. Each experiment was repeated at least three times.

### **3.2.13. 3-(4, 5-methylthiazol-2-yl)-2, 5-diphenyl-tetrazolium-bromide Assay**

To assess cell proliferation, the MTT (3-(4, 5-methylthiazol-2-yl)-2, 5-diphenyl-tetrazolium-bromide) test was used. Human Umbilical Vein Endothelial Cells (HUVECs), mouse neuroblastoma cells (N2a) and human Schwann cells (HSCs) were seeded in triplicates at a density of 5000 cells/well in 96-well plates in a volume of 100 µl in endothelial cell growth medium, Dulbecco's modified Eagle's medium and in Neurobasal medium, respectively. Twelve hours later, the original medium was changed to the 100 µl of siRNA-transfected MiaPaCa-2 or Panc1 supernatants. Negative control siRNA-transfected samples were used as control. After 24 or 48h of incubation, 20µl/well MTT (5mg/ml) was added for 4h. Formazan crystals were

solubilized with 100µl acidic isopropanol. Optical density was measured at 570nm. The read-outs were corrected for the individual day-0 growth. All experiments were repeated three times.

#### **3.2.14. Quantitative Image Analysis**

An automated image analysis system was used on tissue sections without counterstaining to quantify the specific staining. The slides were scanned with the Nikon coolscan V at 4000 dots per inch. The digital images were analyzed in single color for the total surface area (in pixels) versus the stained area. The upper and the lower input levels were overlapped to create black or white images without an intermediate zone. The ideal sensitivity of detection was achieved when the point of overlap corresponded to the vertex of the initial exponential phase of the histogram curve. Results were expressed as percent of the whole scanned section[59, 98].

#### **3.2.15. Densitometry**

Immunoblots were scanned using the Canon 9900F (Tokyo, Japan) scanner. Densitometric analyses were performed using the ImageJ program provided by the NIH. Optic densities from independent experiments were corrected for the individual background noise and the matching equal loading densities (for the cell lysates).

#### **3.2.16. Statistics**

Graphs were created and statistical analyses were performed using the GraphPad Prism 5 software (GraphPad, San Diego, CA). Kaplan-Meier and Log-Rank analyses were used to compare the survival status of the patients. Mann Whitney-U test,



paired t test and Chi-square tests were used for non-categorical and categorical data comparisons. The level of statistical significance was set at 5%.

## 4. RESULTS

### 4.1. Assessment of PEDF Expression in Pancreatic Tissues

Quantitative real-time polymerase chain reaction (QRT-PCR) was performed to evaluate PEDF mRNA expression in bulk tissues of the normal pancreas and PDAC. There was no statistically significant difference between normal pancreatic (n=19) and PDAC (n=20) samples (Figure 1).

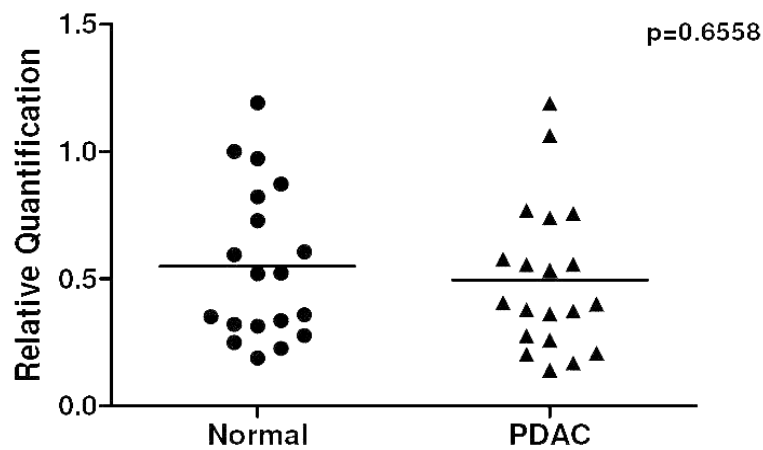


**Figure 1 Expression of PEDF in Normal Pancreas and PDAC.** Expression of PEDF mRNA was analyzed in normal pancreas (n=19) and PDAC (n=20). Real-Time PCR was performed with the LightCycler 480 DNA SYBR Green I Master kit. The target concentration was expressed as a ratio relative to the expression of the reference gene ( $\beta$ -actin) in the same sample and normalized to the calibrator sample.

### 4.2. Localization of PEDF in Pancreatic Tissues

To detect the site specific expression of PEDF protein in pancreatic tissues, immunohistochemical analysis with an anti-PEDF antibody was performed. In the normal pancreas, weak to moderate PEDF immunoreactivity was detected in the cytoplasm of most of the acinar and ductal cells.

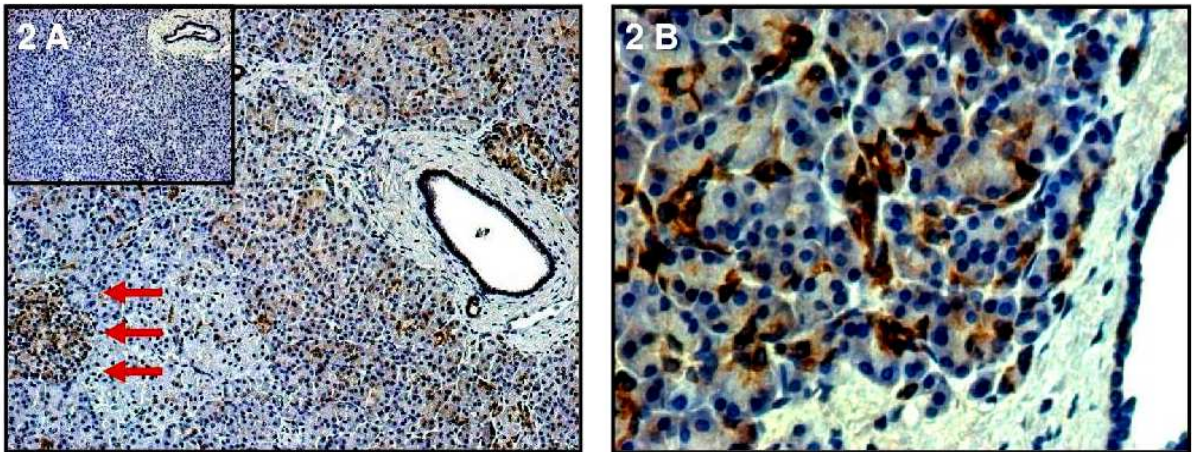


**Figure 2 The Localization of PEDF in Normal Pancreas by IHC.** Immunohistochemical analysis was performed using paraffin-embedded tissue sections of normal pancreas. The staining with anti-PEDF antibody revealed weak to moderate immunoreactivity in the cytoplasm of most of the acinar and ductal cells (2A, 50X; 2B, 200X). Islets displayed strong immunoreactivity to PEDF (2A, red arrows). Negative control is shown as inset.

Some acinar cells displayed stronger PEDF expression (Figure 2A, 2B). Strong immunoreactivity was also detected in the cytoplasm of the islets (Figure 2A).

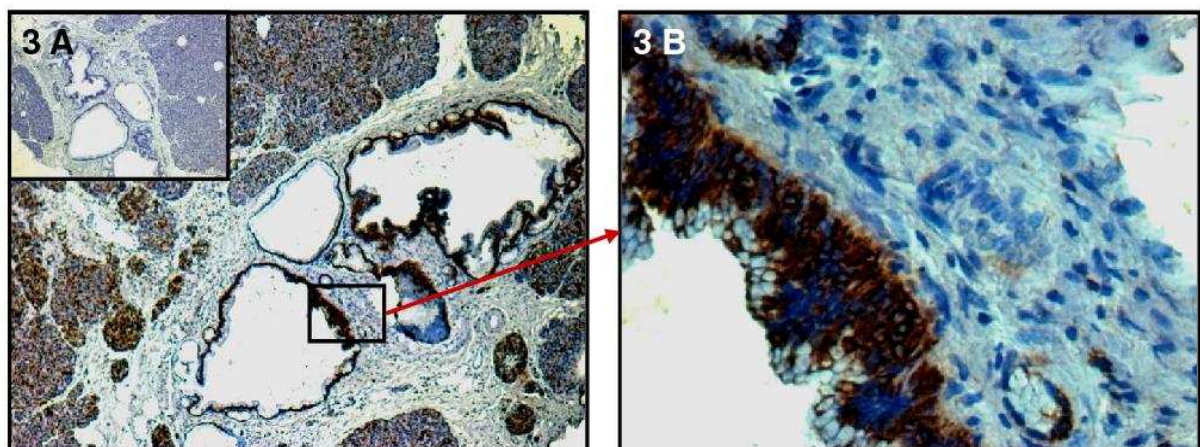


**Figure 3 The Localization of PEDF in the Diseased Pancreas by IHC.** Immunohistochemical analysis of pancreatic tissues was performed using anti-PEDF antibody, with hematoxylin counterstaining. The normal and degenerating acini, metaplastic ductal cells and tubular complexes

seen within the activated stroma in chronic pancreatitis like changes around the cancer were intensely stained (3A, 50X; 3B, 200X). Negative control is shown as inset.

The normal and degenerating acini, hyperplastic ductal cells and tubular complexes seen within the activated stroma in chronic pancreatitis like changes around the cancer were intensely stained (Figure 3A, 3B).

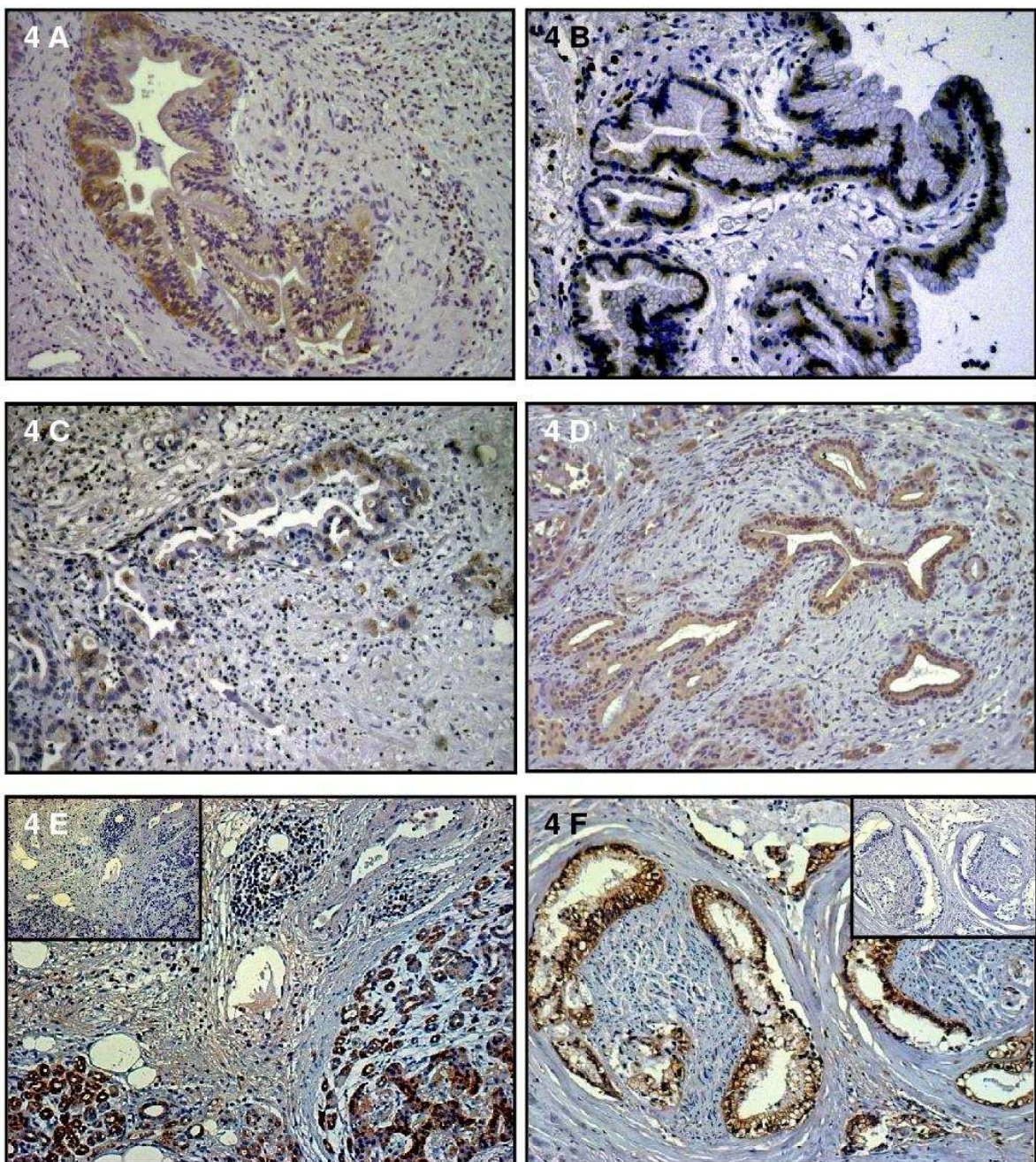


**Figure 4 The Localization of PEDF in PDAC by IHC.** 3µm thick consecutive sections of PDAC (n=55) were immunostained using anti-PEDF antibody with hematoxylin counterstaining. Inflammatory cells and several PanIN lesions exhibited strong immunoreactivity for PEDF (4A, 50X; 4B, 100X; 4E, 100X). Various levels of diffuse cytoplasmic staining were detected in the cancer cells of the all evaluated PDAC specimens (4C, 100X; 4D, 100X; 4F, 100X). Negative controls are shown as insets.

Similarly, several PanIN lesions and most of the inflammatory cells of the cancer tissue exhibited strong immunoreactivity for PEDF (Figure 4A, 4B, 4E). The normal ductal cells in the hypoxic peritumoral areas also displayed increased expression of PEDF compared to the ducts of the normal pancreas. None of the samples displayed PEDF staining of pancreatic stellate cells.

Various levels of diffuse cytoplasmic staining were detected in the cancer cells of the all evaluated PDAC specimens (Figure 4C, 4D, 4F). Among 55 PDAC sections, 85% showed weak to moderate immunoreactivity whereas 15% showed strong immunoreactivity for PEDF.

#### **4.3. Correlation of PEDF Expression in Cancer Cells and Patient Survival**

Fifty-five patients with known survival data were divided into two groups according to their PEDF immunoreactivity. Briefly, the expression scores were calculated by multiplying the values of staining intensity (1 = no staining, 2 = weak/moderate, 3 = strong) with stained area (1 = <33% of the cancer cells, 2 = 33-66% of the cells, 3 = >66% of cancer cells). The survival analysis of these patients revealed a statistically significant correlation between high PEDF expression and longer survival of PDAC patients (p=0.043). The median survival of the patients with low PEDF expression (n=47) was 17 months, whereas 22 months in the patients with high PEDF expression (n=8, Hazard Ratio= 2.634, 95% CI of ratio = 1.021 – 4.855) (Figure 5).

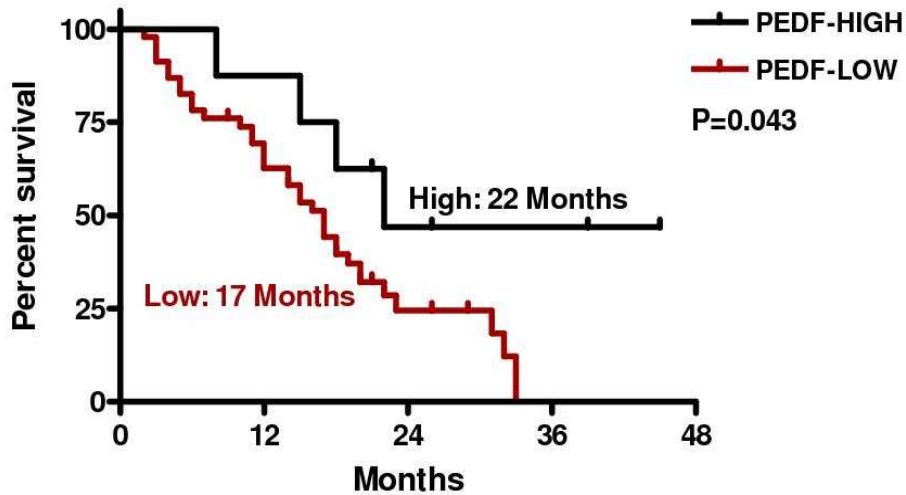


**Figure 5 Correlation of PEDF Expression in Cancer Cells with Survival of the Patients.** 55 PDAC patients with known survival data were divided into two groups according to their PEDF immunoreactivity. Kaplan-Meier survival analysis was performed to compare patient survival status between high and low PEDF expression.

#### 4.4. Correlation of PEDF Expression with Microvessel- and Neural-Density in Pancreatic Cancer

Microscopically there was a reduction of the microvessel density in pancreatic cancer, whereas the number of the hypertrophic nerves dramatically increased (Figure 6A, 6B).

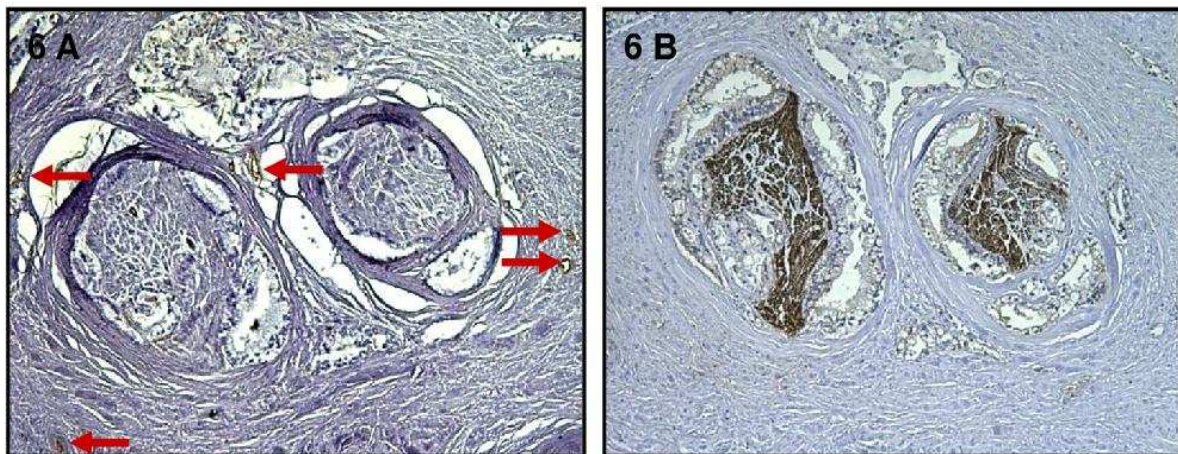


**Figure 6 Correlation of PEDF Expression in Cancer Cells with Microvessel Density and Intrapancreatic Neuropathy.** Immunohistochemical analysis was performed using paraffin-embedded tissues sections of PDAC. The sections were stained with anti-CD31 antibody for endothelial cells (6A) and anti-GAP-43 antibody for intra-pancreatic nerves (6B). IHC revealed the scarcity of the MVD (6A) (red arrows) and increased neuropathy (6B).

Considering the PEDF's known antiangiogenic and neurotrophic activities and higher focal expression in cancer, we analyzed the correlation between the PEDF expression of cancer cells and microvessel- / neural-densities of respective specimens. Endothelial cells were detected by immunohistochemistry using an anti-CD31 antibody that showed no cross reactivity with other cells (Figure 6A, 8A, 8C, 8E).

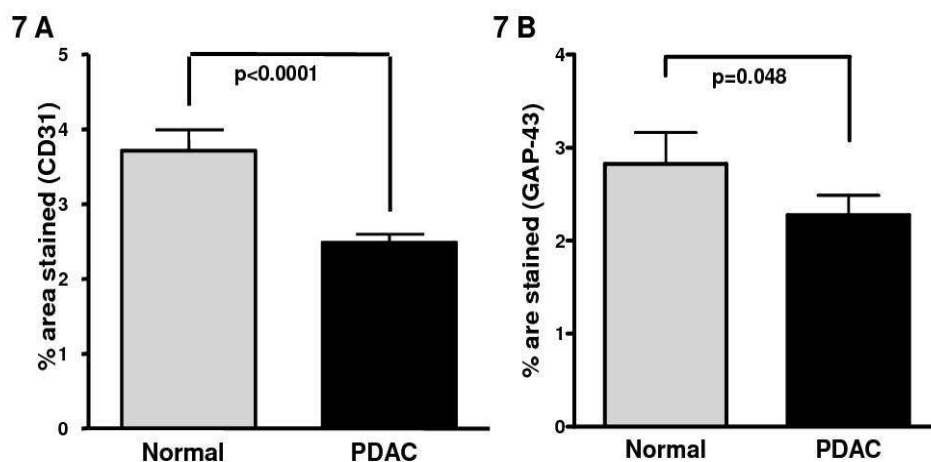


**Figure 7 Microvessel- and Nerve Density in the normal pancreas and PDAC.** Immunohistochemical analysis was performed using paraffin-embedded tissues sections of normal pancreas (n=20) and PDAC (n=55). The sections were stained with anti-CD31 (7A) and anti-GAP-43 antibodies for (7B) without hematoxylin counterstaining to yield better quantification of microvessel- and nerve-densities, respectively. An automated image analysis system was used on tissue sections to quantify the specific staining. Results were expressed as percent of the whole scanned section.

Twenty four patients (44%) exhibited low PEDF and a high MVD (more than the median MVD), while 23 patients (42%) showed a low MVD and low PEDF expression. Four cases (7%) displayed high expression of PEDF and a low MVD, whereas the other 4 patients (7%) exhibited high MVD and high PEDF expression. Although there was a significant decrease (33%,  $p < 0.0001$ ) in the MVD in PDAC compared to the normal pancreas (Figure 6A, 7A, 8A, 8C, 8E), no statistically significant association between PEDF expression and the MVD was found ( $p = 0.96$ ) (Table 2).

		PEDF Expression		
		LOW	HIGH	
CD31 Expression	LOW	23	4	27
	HIGH	24	4	28
		47	8	55
<b>P=0.9556</b>				
		PEDF Expression		
		LOW	HIGH	
GAP43 Expression	LOW	26	1	27
	HIGH	21	7	28
		47	8	55
<b>P=0.0251</b>				

**Table 2 Correlation of PEDF Expression with Microvessel- and Nerve Density in PDAC.** Chi-square analysis was performed for statistical analysis of PEDF, CD31 and GAP43 expressions of 55 PDAC patients. No statistically significant association between PEDF expression and MVD was found ( $p = 0.9556$ ). In contrast, a positive correlation was detected between high PEDF expression and increased nerve density ( $p = 0.0251$ ).



Similarly, a nerve specific anti-GAP-43 antibody that did not cross-react with any other structure was used to assess the nerve-density (Figure 6B, 8B, 8D, 8F).

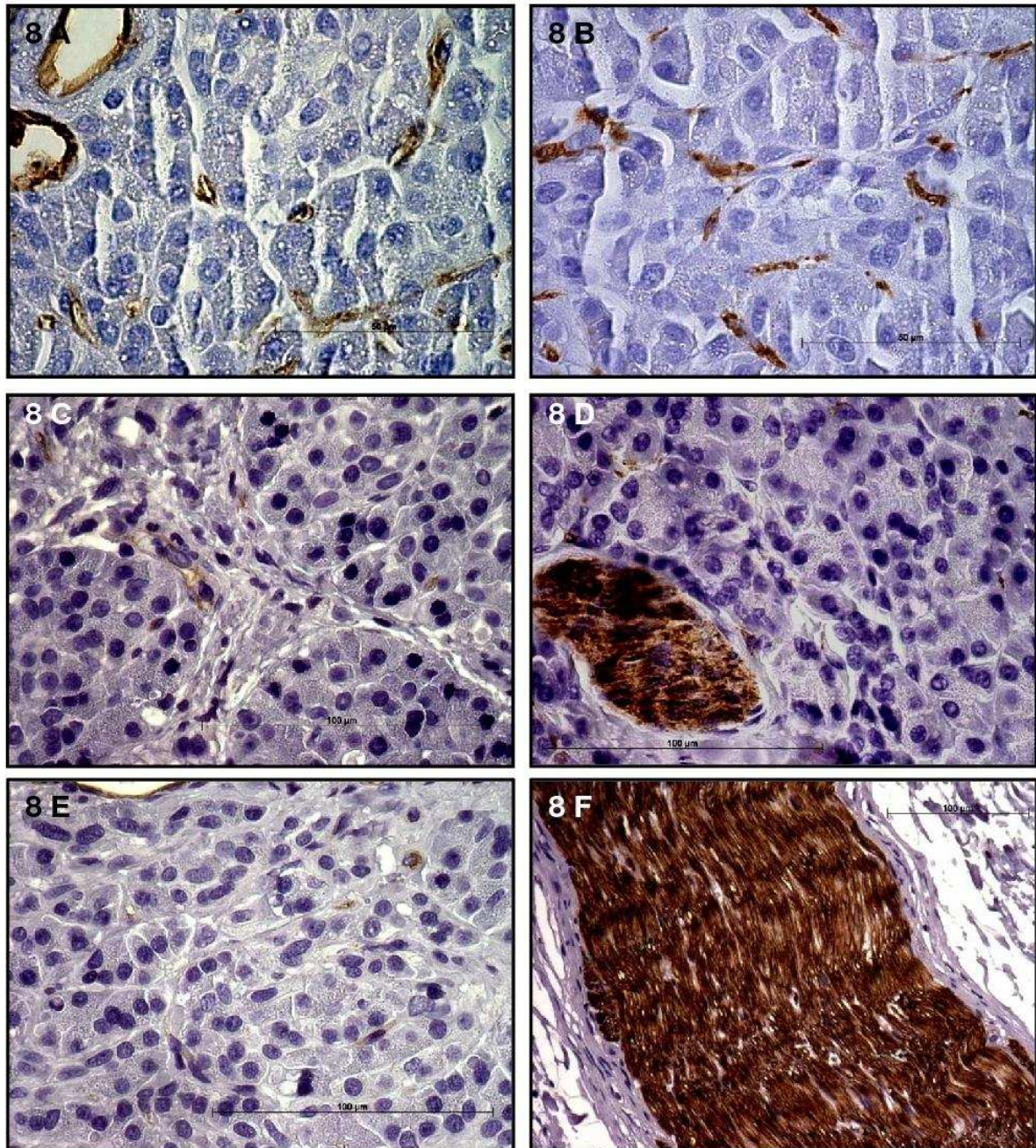


**Figure 8 Reduction of Microvessel- and Nerve-densities on the Activated Stoma of Pancreatic Cancer.** Immunohistochemical analysis was performed using paraffin-embedded tissues sections of normal pancreas (8A, 8B) and normal tissue around PDAC where stromal activity begins (8C, 8D, 8E, 8F). The sections were probed with anti-CD31 antibody for endothelial cells (8A, 8C, 8E) and anti-GAP-43 antibodies for intra-pancreatic nerves (8B, 8D, 8F). Original magnifications 400X.

Although several hypertrophic nerves were seen in PDAC (Figure 6B, 8D, 8F), overall nerve density of the normal pancreas was significantly higher than that of PDAC (20%,  $p=0.048$ ) (Figure 7B).

This reduction of the nerve density and total GAP-43-stained area in PDAC was due to the loss of the fine nerve fibers seen in the periacinar spaces (Figure 8B, 8D).

There was a positive correlation between high PEDF expression of cancer cells and increased nerve caliber and neuropathy in PDAC sections ( $p=0.0251$ ) (Table 2).

#### **4.5. Expression and Localization of PEDF Receptors in Pancreatic Cancer Tissues and Stellate Cells**

Next, the expression of both PEDF receptors, Laminin-R and PNPLA2, was analyzed in pancreatic tissues by immunohistochemistry. Strong cytoplasmic staining for Laminin-R was observed in all cancer cells, PanIN lesions and tubular complexes (Figure 9A). In consecutive sections, the same structures showed a weaker immunoreactivity for PNPLA2 (Figure 9B). Moderate expression of both proteins was detected in inflammatory cells in PDAC tissues. Intrapancreatic nerves displayed moderate and weak staining for Laminin-R and PNPLA2, respectively (Figure 9A, 9B).

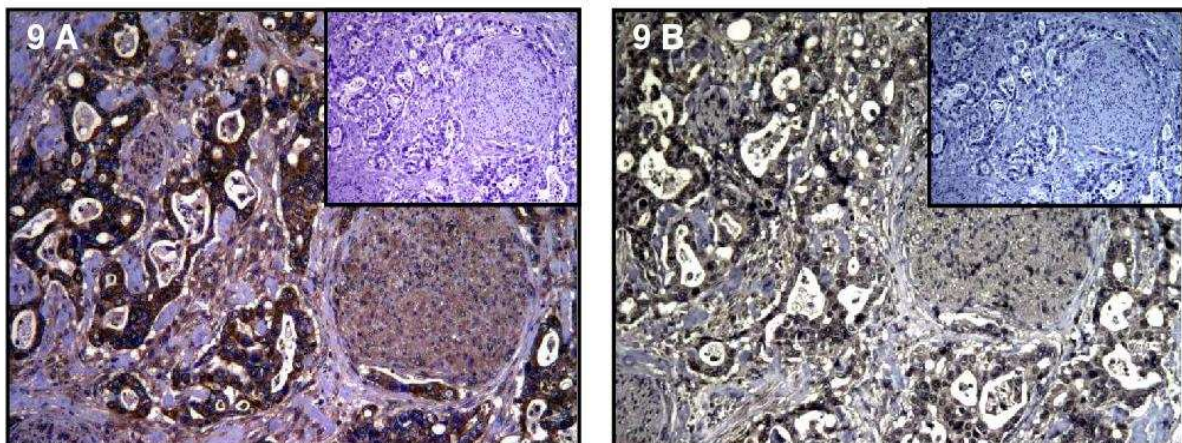


**Figure 9 Expression of PEDF Receptors in PDAC.** Immunohistochemical analysis of PDAC tissues was performed using anti-Laminin-R and anti-PNPLA2 antibodies with hematoxylin counterstaining. Strong cytoplasmic staining for Laminin-R and weak to moderate immunoreactivity for PNPLA2 was revealed in the cancer cells (9A, 9B). Intrapancreatic nerves displayed moderate staining and weak for PNPLA2 (9A, 9B). Negative controls are shown as insets. Original magnifications 100X.

PSC were strongly positive for Laminin-R (Figure 10A). PNPLA2 expression was generally weaker where some PSC remained immunonegative (Figure 10B).

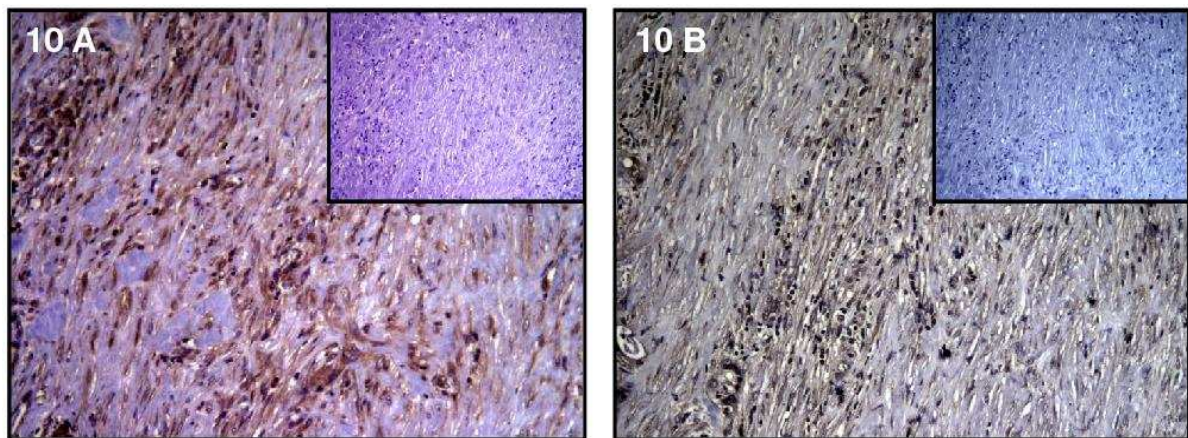


**Figure 10 Expression of PEDF Receptors in PSCs.** Immunohistochemical analysis was performed using anti-Laminin-R and anti-PNPLA2 antibodies with hematoxylin counterstaining. PSCs exhibited strong to moderate immunopositivity for Laminin-R (10A) and staining for PNPLA2 (10B). Negative controls are shown as insets. Original magnifications 100X.

Concordantly, immunofluorescence analysis of cultured human primary PSC showed strong positivity for Laminin-R (Figure 11A), and weaker immunopositivity for PNPLA2, where more than half of the cells remained non-stained (Figure 11B).

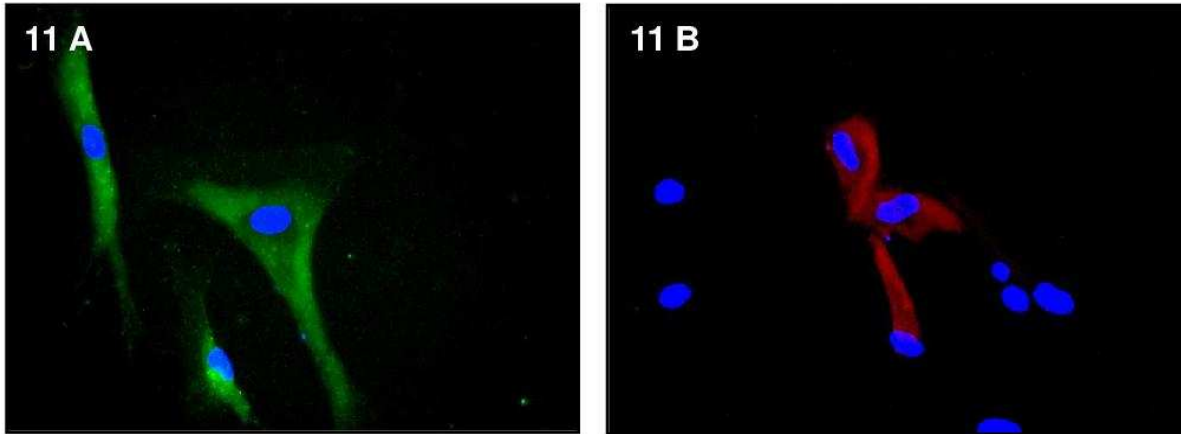


**Figure 11 Expression of PEDF Receptors in PSCs.** PSCs were seeded on Teflon-coated slides at a density of 5000/well in 100 $\mu$ l SM 10%. Twenty-four hours later, cells were fixed with 4% paraformaldehyde, permeabilized with 0.1% Triton X-100, and incubated with anti-Laminin-R and anti-PNPLA2 antibodies overnight at 4 $^{\circ}$ C. The secondary antibodies and DAPI were used appropriately. Immunofluorescence analysis revealed strong expression of Laminin-R (11A) whereas moderate expression of PNPLA2 was detected only in some PSCs (11B). Original magnifications 200X.

#### 4.6. Effects of PEDF on Pancreatic Stellate Cell Activity and Extracellular Matrix Protein Production

Early activation of PSC occurs in the activated stroma between the normal parenchyma and the cancerous areas[59]. This PSC activity leads to the deposition of extracellular matrix proteins in the periacinar spaces (Figure 12A, 12B).

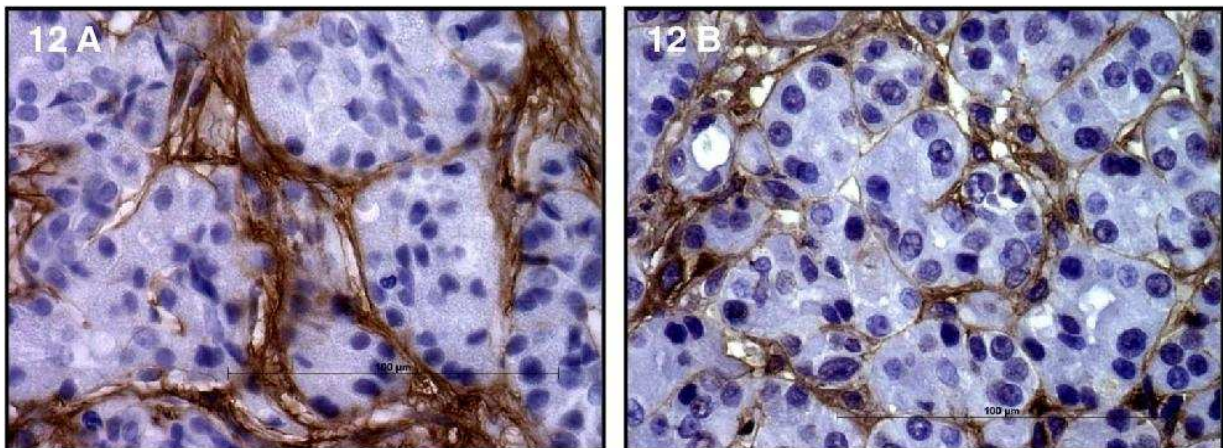


**Figure 12 Periacinar Fibrosis on the Activated Stroma around the Pancreatic Cancer.** Immunohistochemical analysis was performed using paraffin-embedded tissues sections of normal normal tissue around PDAC where stromal activity begins. Anti-periostin antibody was used to detect the early activation of PSC in the periacinar spaces (12A, 400X) and anti-fibronectin antibody for extracellular matrix deposition (12B, 400X).

Since there was a significant overexpression of PEDF on the activated front of the stroma, we analyzed the effect of PEDF on stellate cell activity.

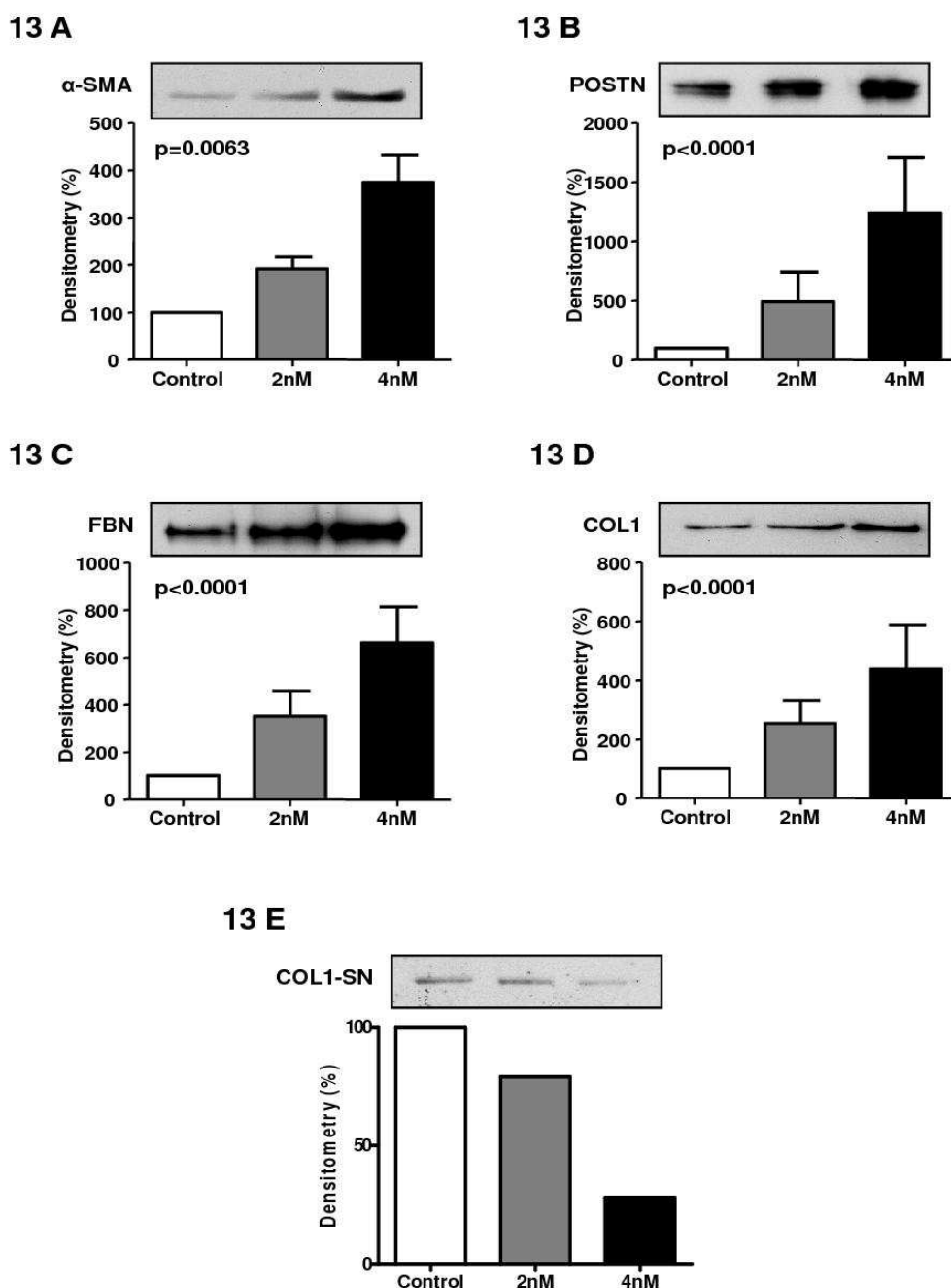


**Figure 13 Effects of recombinant PEDF on Pancreatic Stellate Cells.** Sister clones of PSCs were grown in 6-well plates to 80% confluence. After 24h, fresh SF-LGM containing 0, 2 or 4 nM recombinant human PEDF was added. Immunoblot analysis was performed as described in Materials and Methods section. Probing of the 72h treated cell lysates for  $\alpha$ -SMA (13A) and collagen-type Ia (13D) and the matching SNs for POSTN (13B), fibronectin (13C) and collagen-type Ia (13E). The densitometry analyses are presented as percent change compared with control. Error bars show the SEM of three experiments.

Treatment of PSC with 2nM and 4nM recombinant PEDF protein (rPEDF) increased the  $\alpha$ -SMA expression, 91% and 275%, respectively ( $p=0.0063$ ) (Figure 13A). To assess the stimulatory effect of PEDF on extracellular matrix (ECM) protein synthesis and secretion, the amounts of periostin, collagen-type Ia and fibronectin was assessed in the matching supernatants. Immunoblot analysis revealed a 390% increase in periostin- and 253% increase in fibronectin expression when treated with 2 nM rPEDF. Cells treated with 4nM rPEDF displayed a 1140% and 561% increase of periostin ( $p<0.0001$ ) and fibronectin ( $p<0.0001$ ) expression in PSC supernatants, respectively (Figure 13B and 13C). Although there was a 155% (2 nM) and 338% (4 nM) increase in collagen-type Ia expression in the cell lysates ( $p<0.0001$ ) (Figure 13D), there was a dose dependent reduction in the amount of collagen secreted in the supernatants (Figure 13E).

#### **4.7. Regulation of PEDF Expression in Pancreatic Cancer and Immortalized Duct Cell lines by Oxygen**

It is known that an aberrant deposition of ECM in the periacinar spaces of the normal acini leads to reduced MVD and hypoxia in PDAC [59]. Therefore, the effect of hypoxia on eight pancreatic cancer cell lines and immortalized human pancreatic duct epithelial (HPDE) cells was assessed. The hypoxic state of the cells was

verified by immunoblotting the cell lysates for Hypoxia-Inducible Factor-1  $\alpha$  (Figure 14).

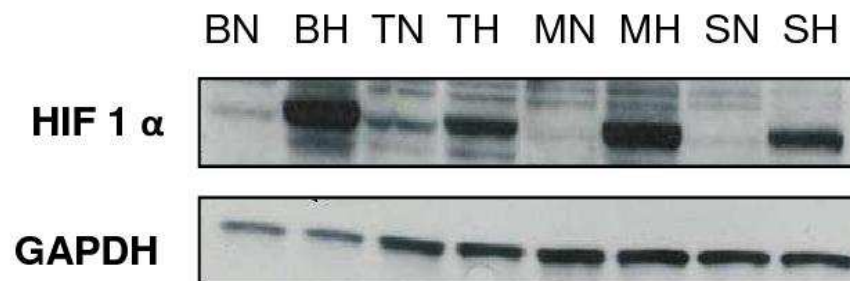


**Figure 14 Verification of hypoxia.** BxPc-3 (B), T3M4 (T), MiaPaCa-2 (M), SU86.86 (S) cell monolayers were incubated in the modular chamber under a hypoxic gas mixture for 16h at 37°C. The sister clones of the hypoxic (H) cells were incubated under normoxic (N) conditions for the same period of time, at 37°C in a humid chamber, saturated with 5% CO<sub>2</sub>. Cells were lysed with lysis buffer for immunoblot analysis. Samples containing 20  $\mu$ g of the protein extract were size-fractionated by 10% SDS-PAGE and transferred onto nitrocellulose membranes by the application of 30 V for 75 minutes. Blots were blocked with 20ml TBS-T plus 5% non-fat milk for 20 min., incubated with the anti-Hypoxia-Inducible Factor-1  $\alpha$  (HIF-1  $\alpha$ ) antibody overnight at 4°C, washed with TBS-T, and incubated with the appropriate secondary antibodies for two hour at room temperature. After washing with TBS-T, antibody detection was performed using the enhanced chemoilluminescence (ECL) reaction system. Equal loading was verified with GAPDH by stripping and reblotting the membrane.

Hypoxia induced the PEDF mRNA expression in seven out of eight pancreatic cancer cell lines and in HPDE cells (Figure 15). However, at the protein level, there was a paradoxical reduction of PEDF protein detected in the supernatants of the matching cells (Figure 16). For example the increase of PEDF mRNA in hypoxic Panc1 was 1040% ( $p=0.0065$ ), whereas PEDF protein was 41% ( $p=0.0044$ ) less in the supernatant of the same cell line, compared with the normoxic controls.

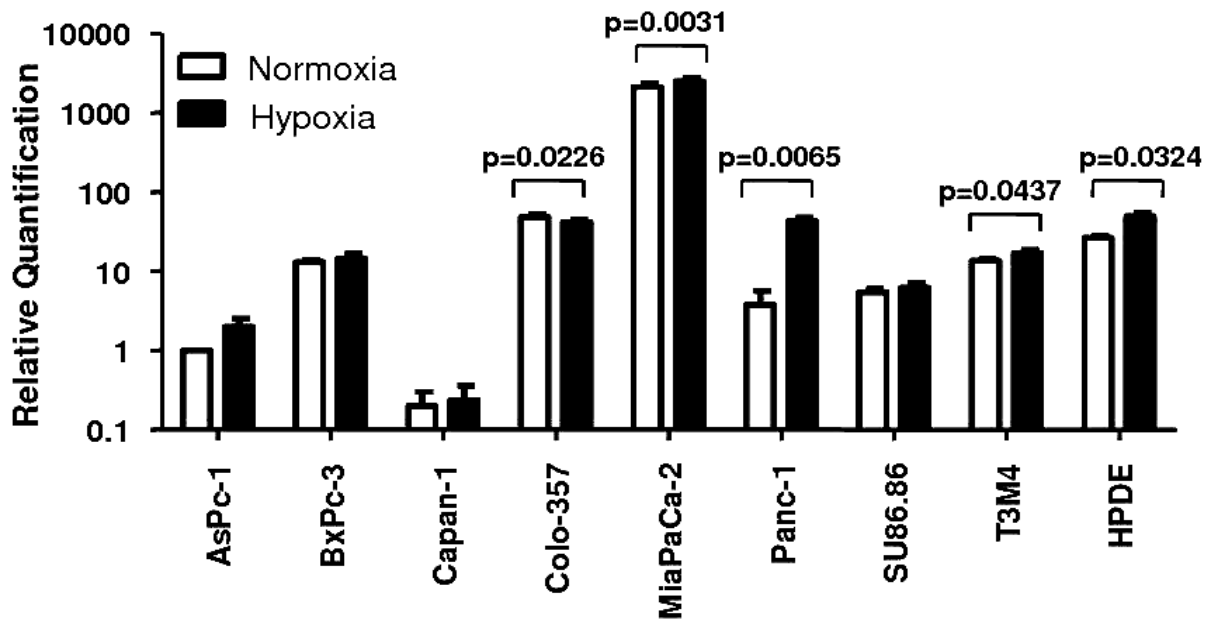


**Figure 15 Effect of Hypoxia on PEDF Expression of Pancreatic Cancer- and Pancreatic Ductal-Cells.** The cells were maintained in the modular chamber under a hypoxic gas mixture (89.25% N<sub>2</sub>, 10% CO<sub>2</sub>, 0.75%O<sub>2</sub>) for 12h at 37°C. QRT-PCR analysis was performed with the LightCycler 480 DNA SYBR Green I Master kit. The target concentration was expressed relative to the concentration of the reference gene ( $\beta$ -actin) in the same sample and normalized to the calibrator sample. Error bars show the SEM of three experiments.

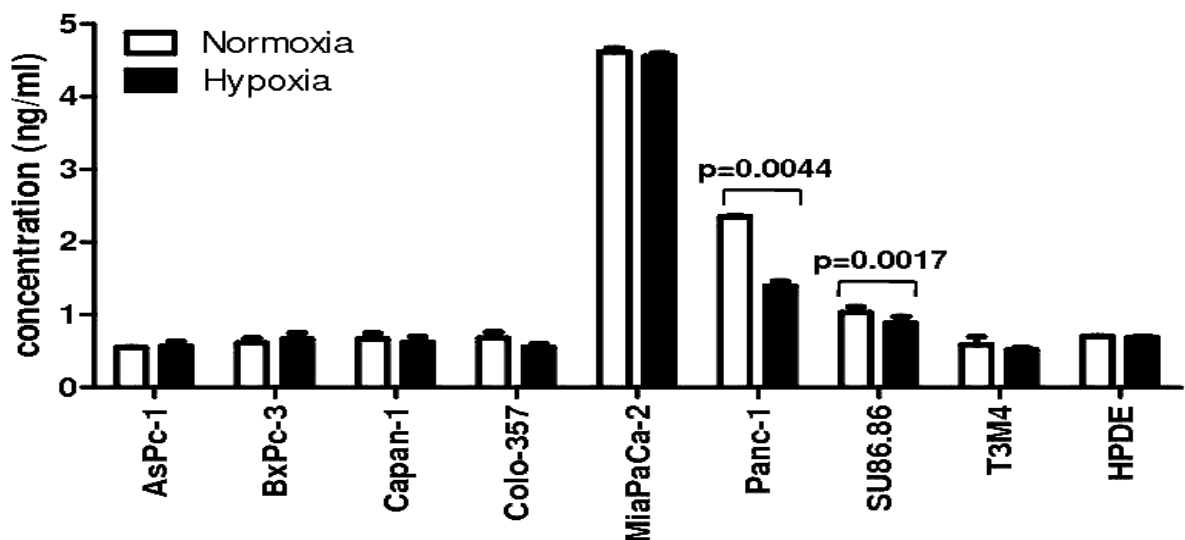


**Figure 16 Effect of Hypoxia on PEDF Expression of Pancreatic Cancer- and Pancreatic Ductal-Cells.** The cells were maintained in the modular chamber under a hypoxic gas mixture (89.25% N<sub>2</sub>, 10% CO<sub>2</sub>, 0.75%O<sub>2</sub>) for 24h at 37°C. Commercial ELISA kit was used to measure PEDF protein in



normoxic and hypoxic supernatants, according to the manufacturer's instructions. Error bars show the SEM of three experiments.

#### 4.8. The Effect of Pancreatic Cancer Cell Supernatants with and without PEDF-silencing on Endothelial Cell Growth

Pancreatic cancer cells exert a dominantly antiangiogenic effect on endothelial cells [59]. To evaluate the contribution of PEDF secretion on the antiangiogenic attributes of pancreatic cancer cells, we tested the growth of human umbilical vein endothelial cells (HUVECs) treated with pancreatic cancer cell supernatants after silencing PEDF in cancer cells by siRNA transfection.

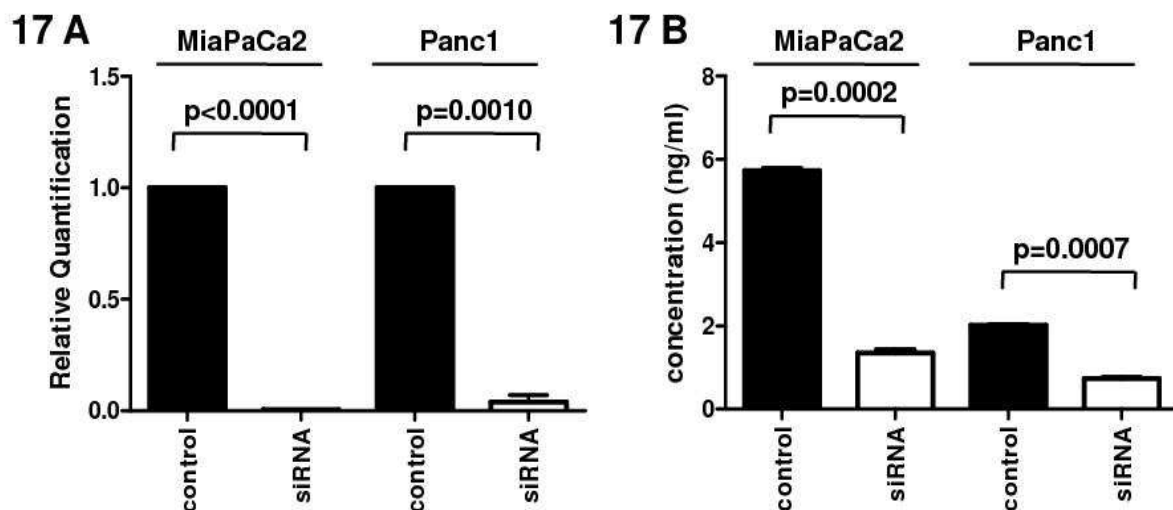


**Figure 17 Effect of PEDF siRNA on Pancreatic Cancer Cells.** MiaPaCa-2 and Panc1 cells were seeded in 6-well plates ( $2.5 \times 10^5$  cells/well) in 2.5 ml of complete medium. 24h later, 10 nM specific PEDF siRNA or negative control siRNA was added. After 24h, total cellular RNA was isolated. QRT-PCR analysis (17A) was performed with the LightCycler 480 DNA SYBR Green I Master kit. The target concentration was expressed relative to the concentration of the reference gene ( $\beta$ -actin) in the same sample and normalized to the calibrator sample. (17B) Commercial ELISA kit was used to measure PEDF protein in the cancer cell supernatants, collected 96h after transfection, according to the manufacturer's instructions. Error bars show the SEM of three experiments.

QRT-PCR analysis demonstrated a significant decrease of the PEDF mRNA in MiaPaCa-2 (99.52%) ( $p < 0.0001$ ) and Panc1 (96.12%) ( $p = 0.0010$ ) cell-lines, when compared with negative control siRNA transfected cells (Figure 17A). The PEDF-silenced MiaPaCa-2 (76.5%,  $p = 0.0002$ ) and Panc1 (63.7%,  $p = 0.0007$ ) also displayed less PEDF protein in their supernatants compared with controls (Figure 17B).

Compared to controls, there was a 21% and 27% reduced inhibition of HUVEC growth when treated with PEDF silenced supernatants of MiaPaCa-2 ( $p = 0.0067$ ) and Panc1 (ns) cells respectively (Figure 18).

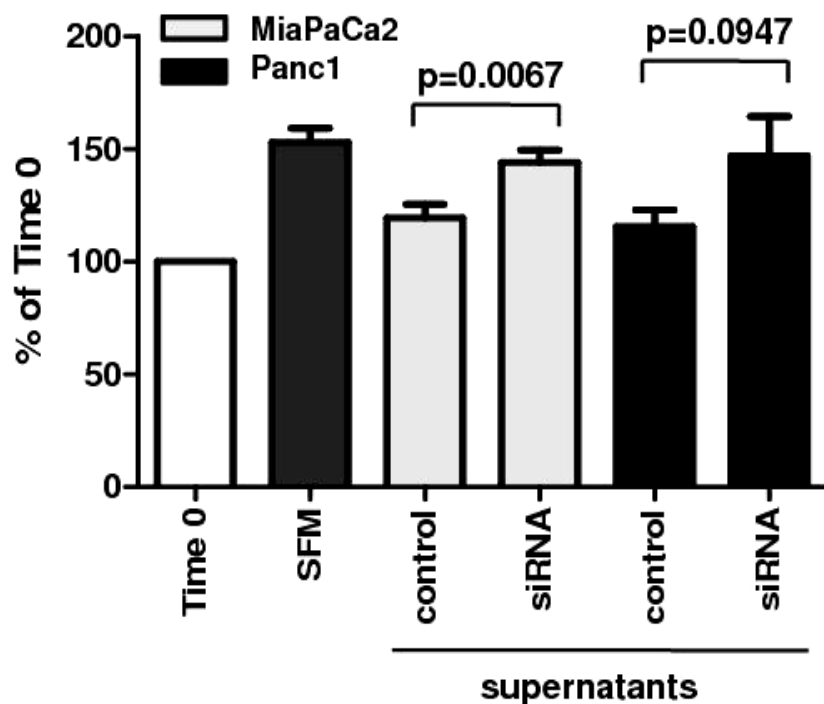


**Figure 18 Effect of PEDF Secreted by Cancer Cells on Endothelial Cell Proliferation.** HUVECs were seeded at a density of 5000 cells/well in 96-well plates. 12h later, 100  $\mu$ l of siRNA-transfected MiaPaCa-2 and Panc1 supernatants was added. Negative control siRNA transfected supernatants were used as control. After 48 hours, 20 $\mu$ l/well MTT (5mg/ml) was added for 4h. Formazan products

were solubilized with 100µl acidic isopropanol. Optical density was measured at 570nm. Error bars show the SEM of three experiments.

#### 4.9. The Effect of Pancreatic Cancer Cell Supernatants with and without PEDF-silencing on Nerve Cell Proliferation

For evaluation of the neuroproliferative effect of PEDF, mouse neuroblastoma cells (N2a) and human Schwann cells were treated with the supernatants of MiaPaCa-2 and Panc1 cells. Compared with controls, there was a 20% and 25% decrease of N2a cell proliferation when treated with the PEDF-silenced supernatants of MiaPaCa-2 ( $p=0.0184$ ) and Panc1 (ns) respectively (Figure 19).

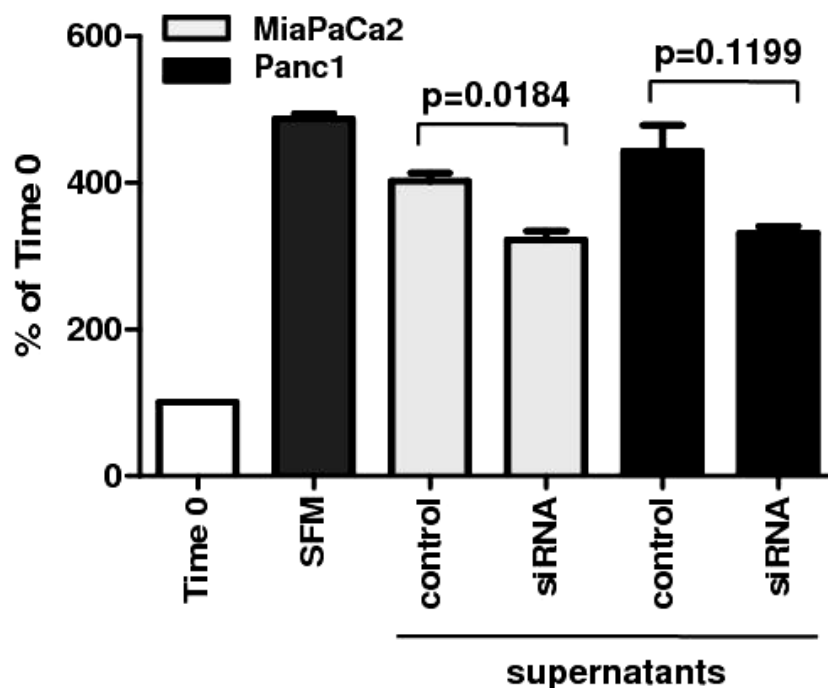


**Figure 19 Effect of PEDF Secreted by Cancer Cells on Neural Cell Proliferation.** N2a cells were seeded at a density of 5000 cells/well in 96-well plates. Twelve hours later, cells were treated with 100 µl of siRNA-transfected MiaPaCa-2 and Panc1 supernatants. Negative control siRNA transfected supernatants were used as control. After 48 hours of incubation, 20µl/well MTT (5mg/ml) was added

for 4 hours. Formazan products were solubilized with 100µl acidic isopropanol. Optical density was measured at 570nm. Error bars show the SEM of three experiments.

There was no significant effect of PEDF-silencing in cancer cells on the growth of human Schwann cells (Figure 20).

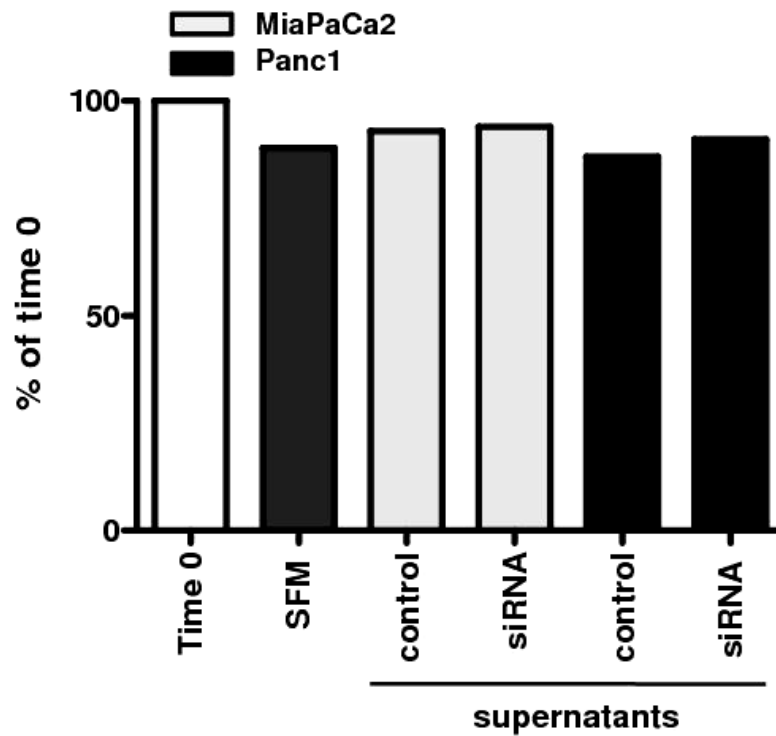


**Figure 20 Effect of PEDF Secreted by Cancer Cells on Human Schwann Cell Proliferation.** Human Schwann cells were seeded at a density of 5000 cells/well in 96-well plates. After 12h the cells were treated with 100 µl of siRNA-transfected MiaPaCa-2 and Panc1 supernatants. Negative control siRNA transfected supernatants were used as control. After 48 hours of incubation, 20µl/well MTT (5mg/ml) was added for 4 hours. Formazan products were solubilized with 100µl acidic isopropanol. Optical density was measured at 570nm.

## 5. DISCUSSION

Pancreatic ductal adenocarcinoma is a lethal disease, characterized by a hypoxic and fibrotic stroma with intrapancreatic neuropathy, aggressive invasion of surrounding tissues, and resistance to oncological therapy. Fibrosis is a consequence of stellate cell over-activity [50-51]. Early activation of stellate cells occurs in the periacinar spaces and leads to the reduction of the microvessel density of the normal pancreas [59]. Masamune et al has shown that hypoxia is a strong activator of stellate cells [58]. Therefore hypoxia and fibrosis forms a vicious-cycle and eventually lead to the loss of the normal parenchyma, creating the barren microenvironment of pancreatic cancer. Stromal activity also impacts significantly on tumor behaviour -even more than the lymph-node status of the cancer [57, 59, 72, 98-100].

Pigment Epithelium-Derived Factor (PEDF) is the most potent natural inhibitor of angiogenesis [94]. In pancreatic cancer, high PEDF expression correlates with a better survival [96]. Uehara et al. argue that higher expression of PEDF in pancreatic cancer leads to a reduction in the MVD of the tumor, which decreases metastatic spread to the liver, thereby contributing to a better survival of patients [96]. In line with this, our results show a similar correlation between higher PEDF expression and longer patient survival. Moreover, silencing of PEDF in pancreatic cancer cells results in lesser inhibition of endothelial cell growth in vitro, showing the contribution of PEDF on the antiangiogenic attributes of pancreatic cancer cells. Nevertheless even after silencing of PEDF, pancreatic cancer cells still remain antiangiogenic, confirming the presence of other antiangiogenic factors like endostatin and angiostatin produced by pancreatic cancer cell lines [59, 101].

PEDF is also a potent neurotrophic factor. It has been documented that the biological activities of PEDF is mediated by high affinity interaction of PEDF and its receptors, Laminin receptor and Patatin-like phospholipase domain-containing protein 2 (PNPLA2) [102-103]. Our experiments revealed the expression of the both PEDF receptors by intrapancreatic nerves and since neuropathic changes are commonly seen in pancreatic cancer, we assessed the correlation of PEDF expression and intrapancreatic nerve density and morphology. In comparison to the normal pancreas, there was a significant reduction of nerve density in terms of the number of nerves seen per area. The fine innervation of the normal acini was almost completely lost in the periacinar fibrosis seen in the activated stroma of pancreatic cancer. This loss of fine innervation was so extensive that, although the pathologically hypertrophic nerves seen in pancreatic cancer are several times bigger than the normal nerves, the total GAP34 positive area of the tumors was 20% less than the average of GAP43 staining of the normal pancreas. GAP-43 is expressed by Schwann-cell precursors and nonmyelinating Schwann cells[104-105]. Following nerve injury, adult myelinating Schwann cells also begin to express GAP-43.

This observation may at first glance seem to contradict several reports in the literature where the investigators reported increased neural density and hypertrophy in chronic pancreatitis and pancreatic cancer[73, 106]. However, it should be considered that in our study, the detected decreased nerve density was mainly due to loss of fine parenchymal “terminal nerve fibers”. Possibly, the selected neural markers in other studies like protein gene product 9.5 [72-73, 106] did not allow the visualization of such parenchymal terminal nerve fibers as opposed to the current study. Therefore, increased neural hypertrophy -a common feature of pancreatic

ductal adenocarcinoma- should not be perceived as “increased nerve fiber density” and not be confused with the concomitant loss of intraparenchymal terminal nerve fibers. Hence, PEDF may exert its neurotrophic role in the compensatory induction of neural hypertrophy as a response to such a loss of intraparenchymal terminal nerve fibers.

By immunohistochemistry, it was clearly visible that there was a stronger expression of PEDF in the activated stroma of the pancreas where chronic pancreatitis-like changes form an umbra around the tumor. In these regions, strongest expression of PEDF was consistently found in the tubular complexes, degenerating acini and inflammatory cells. We have previously shown that early activation of stellate cells occurs in the periacinar spaces, and hypoxia forms a vicious cycle with fibrosis [59]. Since PSC express both PEDF receptors, we analyzed the effects of PEDF on pancreatic stellate cells in terms of their activity and fibrogenesis. Our experiments demonstrated first time that PEDF induces PSC over activation in a dose-dependent manner. Treatment of cultured primary human pancreatic stellate cells with recombinant PEDF resulted in increased  $\alpha$ -SMA expression and increased secretion of periostin, collagen-type Ia and fibronectin. PEDF has strong affinity also for collagen type 1 [107], which is the main component of the stroma in PDAC [45, 47, 108]. PEDF becomes immobilized by binding to collagen [107, 109]. This focal accumulation of PEDF in the stroma inhibits neoangiogenesis while triggering stellate cell activity and fibrosis. Therefore, it is likely that the fine innervation of the acini is lost secondary to periacinar fibrosis, reduction of capillary perfusion and ensuing hypoxia [59].

On the other hand, chronic inflammation and neurotrophic factors like PEDF, glial cell line-derived-neurotrophic factor (GDNF) family of ligands (GDNF, Artemin,

Neurturin, Persephin) and, nerve growth factor secreted by inflammatory- and cancer cells are believed to cause intrapancreatic neuropathy seen in chronic pancreatitis and pancreatic ductal adenocarcinoma [73, 110-113]. Therefore, we assessed the influence of high versus lower PEDF expression of cancer cells on neuropathy. There was a statistically significant correlation between higher PEDF expression of cancer cells and enlarged nerves seen in PDAC. Intrapaneatic nerve invasion is a typical feature of pancreatic cancer. Most of the data in the literature so far focuses on secretion of chemoattractants by the nerves that leads to the perineural invasion by cancer cells [110-113] Considering the plasticity and remodelling of nerves in pancreatic cancer [114], it is equally possible that secretion of the neurotrophic protein PEDF by cancer cells may lead to the sprouting of the nerves towards cancer structures, thereby contributing to the neuro-cancer interaction with an alternative mechanism. At the functional level, PEDF seems to exert its effect on neural cells since primary human Schwann-cells were indifferent to PEDF in vitro whereas PEDF increased the proliferation of N2a mouse neuroblastoma cells. This observation is in line with other reports showing that PEDF is a neurotrophic factor, promoting neuronal differentiation and long-term survival maintenance of differentiated neurons in human Y-79 retinoblastoma cells [83-84] and cerebellar granule cells [90]. PEDF has also been reported to protect rat motor neurons against glutamate-induced neurotoxicity[92] and to reduce motor neuron death and prevent atrophy of surviving neurons completely in neonatal mice with axotomized sciatic nerves [115].

It remains still unclear what the reason was for the site-specific upregulation of PEDF on the activated stroma of the PDAC. Although hypoxia strongly induced PEDF mRNA in cancer cells, it was not possible to detect a similar increase in the protein expression. To exclude the possibility of a counteracting mechanism developed in



the pancreatic cancer cells, we also treated immortalized ductal pancreatic cells with hypoxia. Similarly, the 132-fold increase in the PEDF mRNA was not reflected to the protein expression.

In conclusion, focal increased expression of PEDF in pancreatic ductal adenocarcinoma is partly responsible for tissue hypoxia by suppression of angiogenesis. Besides its anti-angiogenic effects, PEDF was identified to exert fibrogenic effects by activating pancreatic stellate cells and promoting extracellular matrix protein production. It is likely that the cumulative effect of fibrosis and hypoxia in the periacinar spaces overwhelms the neuroprotective effects of PEDF on the fine nerve fibers seen around the normal acini. However, it would be an oversimplification to reduce the neuropathy only to higher or lower expression of PEDF in pancreatic cancer. It is known that other neurotrophic factors like glial cell line-derived neurotrophic factor (GDNF) family of ligands and, nerve growth factor secreted by inflammatory- and cancer cells lead to intrapancreatic neuropathy seen in chronic pancreatitis and pancreatic ductal adenocarcinoma [73, 110-113]. Since PEDF is also a potent neurotrophic and neuroproliferative factor, increased focal expression of PEDF in some of the pancreatic cancer patients correlates also with intrapancreatic neuropathy.

## **6. SUMMARY**

PEDF is the most potent endogenous anti-angiogenic factor with neuroprotective and neuroproliferative functions. Its expression is documented in normal pancreas and in PDAC. Increased expression of PEDF in pancreatic ductal adenocarcinoma significantly correlated with better patient survival and increased PSC activity. Activated pancreatic stellate cells are the main producers of extracellular matrix proteins; hence PEDF exerts fibrogenic effects and thereby is contributed to the desmoplasia of pancreatic cancer. The periacinar fibrosis leads to the degeneration of the fine acinar innervations, seen in normal pancreas and results in increased intrapancreatic neuropathy correlated with increased focal expression of PEDF in some of the pancreatic cancer patients. Besides its fibrogenic, neurotrophic and neuroproliferative effects, expression of PEDF is partly responsible for tissue hypoxia by suppression of angiogenesis in pancreatic cancer.

## 7. REFERENCES

1. Kleeff, J., P. Beckhove, I. Esposito, S. Herzig, P.E. Huber, J.M. Lohr, and H. Friess, *Pancreatic cancer microenvironment*. *Int J Cancer*, 2007. **121**(4): p. 699-705.
2. Jemal, A., R. Siegel, E. Ward, Y. Hao, J. Xu, and M.J. Thun, *Cancer statistics, 2009*. *CA Cancer J Clin*, 2009. **59**(4): p. 225-49.
3. Jemal, A., R. Siegel, E. Ward, T. Murray, J. Xu, and M.J. Thun, *Cancer statistics, 2007*. *CA Cancer J Clin*, 2007. **57**(1): p. 43-66.
4. Jemal, A., A. Thomas, T. Murray, and M. Thun, *Cancer statistics, 2002*. *CA Cancer J Clin*, 2002. **52**(1): p. 23-47.
5. Verslype, C., E. Van Cutsem, M. Dicato, S. Cascinu, D. Cunningham, E. Diaz-Rubio, B. Glimelius, D. Haller, K. Haustermans, V. Heinemann, P. Hoff, P.G. Johnston, D. Kerr, R. Labianca, C. Louvet, B. Minsky, M. Moore, B. Nordlinger, S. Pedrazzoli, A. Roth, M. Rothenberg, P. Rougier, H.J. Schmoll, J. Tabernero, M. Tempero, C. van de Velde, J.L. Van Laethem, and J. Zalcborg, *The management of pancreatic cancer. Current expert opinion and recommendations derived from the 8th World Congress on Gastrointestinal Cancer, Barcelona, 2006*. *Ann Oncol*, 2007. **18 Suppl 7**: p. vii1-vii10.
6. Tersmette, A.C., G.M. Petersen, G.J. Offerhaus, F.C. Falatko, K.A. Brune, M. Goggins, E. Rozenblum, R.E. Wilentz, C.J. Yeo, J.L. Cameron, S.E. Kern, and R.H. Hruban, *Increased risk of incident pancreatic cancer among first-degree relatives of patients with familial pancreatic cancer*. *Clin Cancer Res*, 2001. **7**(3): p. 738-44.

7. Fuchs, C.S., G.A. Colditz, M.J. Stampfer, E.L. Giovannucci, D.J. Hunter, E.B. Rimm, W.C. Willett, and F.E. Speizer, *A prospective study of cigarette smoking and the risk of pancreatic cancer*. Arch Intern Med, 1996. **156**(19): p. 2255-60.
8. Everhart, J. and D. Wright, *Diabetes mellitus as a risk factor for pancreatic cancer. A meta-analysis*. JAMA, 1995. **273**(20): p. 1605-9.
9. Michaud, D.S., E. Giovannucci, W.C. Willett, G.A. Colditz, M.J. Stampfer, and C.S. Fuchs, *Physical activity, obesity, height, and the risk of pancreatic cancer*. JAMA, 2001. **286**(8): p. 921-9.
10. Greer, J.B., D.C. Whitcomb, and R.E. Brand, *Genetic predisposition to pancreatic cancer: a brief review*. Am J Gastroenterol, 2007. **102**(11): p. 2564-9.
11. Groen, E.J., A. Roos, F.L. Muntinghe, R.H. Enting, J. de Vries, J.H. Kleibeuker, M.J. Witjes, T.P. Links, and A.P. van Beek, *Extra-intestinal manifestations of familial adenomatous polyposis*. Ann Surg Oncol, 2008. **15**(9): p. 2439-50.
12. Lynch, H.T. and R.M. Fusaro, *Pancreatic cancer and the familial atypical multiple mole melanoma (FAMMM) syndrome*. Pancreas, 1991. **6**(2): p. 127-31.
13. Petersen, G.M., M. de Andrade, M. Goggins, R.H. Hruban, M. Bondy, J.F. Korczak, S. Gallinger, H.T. Lynch, S. Syngal, K.G. Rabe, D. Seminara, and A.P. Klein, *Pancreatic cancer genetic epidemiology consortium*. Cancer Epidemiol Biomarkers Prev, 2006. **15**(4): p. 704-10.
14. Lowenfels, A.B., P. Maisonneuve, G. Cavallini, R.W. Ammann, P.G. Lankisch, J.R. Andersen, E.P. Dimagno, A. Andren-Sandberg, and L. Domellof,

- Pancreatitis and the risk of pancreatic cancer. International Pancreatitis Study Group. N Engl J Med, 1993. 328(20): p. 1433-7.*
15. Malka, D., P. Hammel, F. Maire, P. Rufat, I. Madeira, F. Pessione, P. Levy, and P. Ruszniewski, *Risk of pancreatic adenocarcinoma in chronic pancreatitis. Gut, 2002. 51(6): p. 849-52.*
  16. Lowenfels, A.B. and P. Maisonneuve, *Epidemiologic and etiologic factors of pancreatic cancer. Hematol Oncol Clin North Am, 2002. 16(1): p. 1-16.*
  17. Hruban, R.H., A.D. van Mansfeld, G.J. Offerhaus, D.H. van Weering, D.C. Allison, S.N. Goodman, T.W. Kensler, K.K. Bose, J.L. Cameron, and J.L. Bos, *K-ras oncogene activation in adenocarcinoma of the human pancreas. A study of 82 carcinomas using a combination of mutant-enriched polymerase chain reaction analysis and allele-specific oligonucleotide hybridization. Am J Pathol, 1993. 143(2): p. 545-54.*
  18. Dang, C.X., Y. Han, Z.Y. Qin, and Y.J. Wang, *Clinical significance of expression of p21 and p53 proteins and proliferating cell nuclear antigen in pancreatic cancer. Hepatobiliary Pancreat Dis Int, 2002. 1(2): p. 302-5.*
  19. Dergham, S.T., M.C. Dugan, R. Kucway, W. Du, D.S. Kamarauskiene, V.K. Vaitkevicius, J.D. Crissman, and F.H. Sarkar, *Prevalence and clinical significance of combined K-ras mutation and p53 aberration in pancreatic adenocarcinoma. Int J Pancreatol, 1997. 21(2): p. 127-43.*
  20. Dong, M., Q. Dong, H. Zhang, J. Zhou, Y. Tian, and Y. Dong, *Expression of Gadd45a and p53 proteins in human pancreatic cancer: potential effects on clinical outcomes. J Surg Oncol, 2007. 95(4): p. 332-6.*
  21. Dugan, M.C., S.T. Dergham, R. Kucway, K. Singh, L. Biernat, W. Du, V.K. Vaitkevicius, J.D. Crissman, and F.H. Sarkar, *HER-2/neu expression in*

- pancreatic adenocarcinoma: relation to tumor differentiation and survival.* Pancreas, 1997. **14**(3): p. 229-36.
22. Hua, Z., Y.C. Zhang, X.M. Hu, and Z.G. Jia, *Loss of DPC4 expression and its correlation with clinicopathological parameters in pancreatic carcinoma.* World J Gastroenterol, 2003. **9**(12): p. 2764-7.
23. Goggins, M., M. Schutte, J. Lu, C.A. Moskaluk, C.L. Weinstein, G.M. Petersen, C.J. Yeo, C.E. Jackson, H.T. Lynch, R.H. Hruban, and S.E. Kern, *Germline BRCA2 gene mutations in patients with apparently sporadic pancreatic carcinomas.* Cancer Res, 1996. **56**(23): p. 5360-4.
24. Friess, H., J. Ding, J. Kleeff, L. Fenkell, J.A. Rosinski, A. Guweidhi, J.F. Reidhaar-Olson, M. Korc, J. Hammer, and M.W. Buchler, *Microarray-based identification of differentially expressed growth- and metastasis-associated genes in pancreatic cancer.* Cell Mol Life Sci, 2003. **60**(6): p. 1180-99.
25. Hu, Y.X., H. Watanabe, K. Ohtsubo, Y. Yamaguchi, A. Ha, T. Okai, and N. Sawabu, *Frequent loss of p16 expression and its correlation with clinicopathological parameters in pancreatic carcinoma.* Clin Cancer Res, 1997. **3**(9): p. 1473-7.
26. Li, Y., M. Bhuiyan, V.K. Vaitkevicius, and F.H. Sarkar, *Molecular analysis of the p53 gene in pancreatic adenocarcinoma.* Diagn Mol Pathol, 1998. **7**(1): p. 4-9.
27. Safran, H., M. Steinhoff, S. Mangray, R. Rathore, T.C. King, L. Chai, K. Berzein, T. Moore, D. Iannitti, P. Reiss, T. Pasquariello, P. Akerman, D. Quirk, R. Mass, L. Goldstein, and U. Tantravahi, *Overexpression of the HER-2/neu oncogene in pancreatic adenocarcinoma.* Am J Clin Oncol, 2001. **24**(5): p. 496-9.

28. Cubilla, A.L. and P.J. Fitzgerald, *Morphological lesions associated with human primary invasive nonendocrine pancreas cancer*. *Cancer Res*, 1976. **36**(7 PT 2): p. 2690-8.
29. Pour, P., J. Althoff, and M. Takahashi, *Early lesions of pancreatic ductal carcinoma in the hamster model*. *Am J Pathol*, 1977. **88**(2): p. 291-308.
30. Mukada, T. and S. Yamada, *Dysplasia and carcinoma in situ of the exocrine pancreas*. *Tohoku J Exp Med*, 1982. **137**(2): p. 115-24.
31. Brockie, E., A. Anand, and J. Albores-Saavedra, *Progression of atypical ductal hyperplasia/carcinoma in situ of the pancreas to invasive adenocarcinoma*. *Ann Diagn Pathol*, 1998. **2**(5): p. 286-92.
32. Kern, S., R. Hruban, M.A. Hollingsworth, R. Brand, T.E. Adrian, E. Jaffee, and M.A. Tempero, *A white paper: the product of a pancreas cancer think tank*. *Cancer Res*, 2001. **61**(12): p. 4923-32.
33. Schwartz, A.M. and D.E. Henson, *Familial and sporadic pancreatic carcinoma, epidemiologic concordance*. *Am J Surg Pathol*, 2007. **31**(4): p. 645-6.
34. Kozuka, S., R. Sassa, T. Taki, K. Masamoto, S. Nagasawa, S. Saga, K. Hasegawa, and M. Takeuchi, *Relation of pancreatic duct hyperplasia to carcinoma*. *Cancer*, 1979. **43**(4): p. 1418-28.
35. Hruban, R.H., N.V. Adsay, J. Albores-Saavedra, C. Compton, E.S. Garrett, S.N. Goodman, S.E. Kern, D.S. Klimstra, G. Kloppel, D.S. Longnecker, J. Luttges, and G.J. Offerhaus, *Pancreatic intraepithelial neoplasia: a new nomenclature and classification system for pancreatic duct lesions*. *Am J Surg Pathol*, 2001. **25**(5): p. 579-86.

36. Hruban, R.H., K. Takaori, D.S. Klimstra, N.V. Adsay, J. Albores-Saavedra, A.V. Biankin, S.A. Biankin, C. Compton, N. Fukushima, T. Furukawa, M. Goggins, Y. Kato, G. Kloppel, D.S. Longnecker, J. Luttges, A. Maitra, G.J. Offerhaus, M. Shimizu, and S. Yonezawa, *An illustrated consensus on the classification of pancreatic intraepithelial neoplasia and intraductal papillary mucinous neoplasms*. Am J Surg Pathol, 2004. **28**(8): p. 977-87.
37. Vinay Kumar, N.F., Abul Abbas, *Robbins & Cotran Pathologic Basis of Disease*. 2004 Saunders. 1552.
38. Wagner, M., C. Redaelli, M. Lietz, C.A. Seiler, H. Friess, and M.W. Buchler, *Curative resection is the single most important factor determining outcome in patients with pancreatic adenocarcinoma*. Br J Surg, 2004. **91**(5): p. 586-94.
39. Li, D., K. Xie, R. Wolff, and J.L. Abbruzzese, *Pancreatic cancer*. Lancet, 2004. **363**(9414): p. 1049-57.
40. Yeo, C.J., J.L. Cameron, T.A. Sohn, K.D. Lillemoe, H.A. Pitt, M.A. Talamini, R.H. Hruban, S.E. Ord, P.K. Sauter, J. Coleman, M.L. Zahurak, L.B. Grochow, and R.A. Abrams, *Six hundred fifty consecutive pancreaticoduodenectomies in the 1990s: pathology, complications, and outcomes*. Ann Surg, 1997. **226**(3): p. 248-57; discussion 257-60.
41. Kalsner, M.H. and S.S. Ellenberg, *Pancreatic cancer. Adjuvant combined radiation and chemotherapy following curative resection*. Arch Surg, 1985. **120**(8): p. 899-903.
42. *Further evidence of effective adjuvant combined radiation and chemotherapy following curative resection of pancreatic cancer. Gastrointestinal Tumor Study Group*. Cancer, 1987. **59**(12): p. 2006-10.



43. Oettle, H., S. Post, P. Neuhaus, K. Gellert, J. Langrehr, K. Ridwelski, H. Schramm, J. Fahlke, C. Zuelke, C. Burkart, K. Gutberlet, E. Kettner, H. Schmalenberg, K. Weigang-Koehler, W.O. Bechstein, M. Niedergethmann, I. Schmidt-Wolf, L. Roll, B. Doerken, and H. Riess, *Adjuvant chemotherapy with gemcitabine vs observation in patients undergoing curative-intent resection of pancreatic cancer: a randomized controlled trial*. JAMA, 2007. **297**(3): p. 267-77.
44. Flanders, T.Y. and W.D. Foulkes, *Pancreatic adenocarcinoma: epidemiology and genetics*. J Med Genet, 1996. **33**(11): p. 889-98.
45. Erkan, M., J. Kleeff, A. Gorbachevski, C. Reiser, T. Mitkus, I. Esposito, T. Giese, M.W. Buchler, N.A. Giese, and H. Friess, *Periostin creates a tumor-supportive microenvironment in the pancreas by sustaining fibrogenic stellate cell activity*. Gastroenterology, 2007. **132**(4): p. 1447-64.
46. Kloppel, G., S. Detlefsen, and B. Feyerabend, *Fibrosis of the pancreas: the initial tissue damage and the resulting pattern*. Virchows Arch, 2004. **445**(1): p. 1-8.
47. Mollenhauer, J., I. Roether, and H.F. Kern, *Distribution of extracellular matrix proteins in pancreatic ductal adenocarcinoma and its influence on tumor cell proliferation in vitro*. Pancreas, 1987. **2**(1): p. 14-24.
48. Bachem, M.G., M. Schunemann, M. Ramadani, M. Siech, H. Beger, A. Buck, S. Zhou, A. Schmid-Kotsas, and G. Adler, *Pancreatic carcinoma cells induce fibrosis by stimulating proliferation and matrix synthesis of stellate cells*. Gastroenterology, 2005. **128**(4): p. 907-21.
49. Vonlaufen, A., S. Joshi, C. Qu, P.A. Phillips, Z. Xu, N.R. Parker, C.S. Toi, R.C. Pirola, J.S. Wilson, D. Goldstein, and M.V. Apte, *Pancreatic stellate*

- cells: partners in crime with pancreatic cancer cells*. Cancer Res, 2008. **68**(7): p. 2085-93.
50. Apte, M.V., P.S. Haber, T.L. Applegate, I.D. Norton, G.W. McCaughan, M.A. Korsten, R.C. Pirola, and J.S. Wilson, *Periacinar stellate shaped cells in rat pancreas: identification, isolation, and culture*. Gut, 1998. **43**(1): p. 128-33.
51. Bachem, M.G., E. Schneider, H. Gross, H. Weidenbach, R.M. Schmid, A. Menke, M. Siech, H. Beger, A. Grunert, and G. Adler, *Identification, culture, and characterization of pancreatic stellate cells in rats and humans*. Gastroenterology, 1998. **115**(2): p. 421-32.
52. Omary, M.B., A. Lugea, A.W. Lowe, and S.J. Pandol, *The pancreatic stellate cell: a star on the rise in pancreatic diseases*. J Clin Invest, 2007. **117**(1): p. 50-9.
53. Apte, M.V., P.S. Haber, S.J. Darby, S.C. Rodgers, G.W. McCaughan, M.A. Korsten, R.C. Pirola, and J.S. Wilson, *Pancreatic stellate cells are activated by proinflammatory cytokines: implications for pancreatic fibrogenesis*. Gut, 1999. **44**(4): p. 534-41.
54. Shek, F.W., R.C. Benyon, F.M. Walker, P.R. McCrudden, S.L. Pender, E.J. Williams, P.A. Johnson, C.D. Johnson, A.C. Bateman, D.R. Fine, and J.P. Iredale, *Expression of transforming growth factor-beta 1 by pancreatic stellate cells and its implications for matrix secretion and turnover in chronic pancreatitis*. Am J Pathol, 2002. **160**(5): p. 1787-98.
55. Phillips, P.A., M.J. Wu, R.K. Kumar, E. Doherty, J.A. McCarroll, S. Park, R.C. Pirola, J.S. Wilson, and M.V. Apte, *Cell migration: a novel aspect of pancreatic stellate cell biology*. Gut, 2003. **52**(5): p. 677-82.

56. Mueller, M.M. and N.E. Fusenig, *Friends or foes - bipolar effects of the tumour stroma in cancer*. Nat Rev Cancer, 2004. **4**(11): p. 839-49.
57. Koong, A.C., V.K. Mehta, Q.T. Le, G.A. Fisher, D.J. Terris, J.M. Brown, A.J. Bastidas, and M. Vierra, *Pancreatic tumors show high levels of hypoxia*. Int J Radiat Oncol Biol Phys, 2000. **48**(4): p. 919-22.
58. Masamune, A., K. Kikuta, T. Watanabe, K. Satoh, M. Hirota, and T. Shimosegawa, *Hypoxia stimulates pancreatic stellate cells to induce fibrosis and angiogenesis in pancreatic cancer*. Am J Physiol Gastrointest Liver Physiol, 2008. **295**(4): p. G709-17.
59. Erkan, M., C. Reiser-Erkan, C.W. Michalski, S. Deucker, D. Sauliunaite, S. Streit, I. Esposito, H. Friess, and J. Kleeff, *Cancer-stellate cell interactions perpetuate the hypoxia-fibrosis cycle in pancreatic ductal adenocarcinoma*. Neoplasia, 2009. **11**(5): p. 497-508.
60. Duffy, J.P., G. Eibl, H.A. Reber, and O.J. Hines, *Influence of hypoxia and neoangiogenesis on the growth of pancreatic cancer*. Mol Cancer, 2003. **2**: p. 12.
61. Harris, A.L., *Hypoxia--a key regulatory factor in tumour growth*. Nat Rev Cancer, 2002. **2**(1): p. 38-47.
62. Salvioli, B., M. Bovera, G. Barbara, F. De Ponti, V. Stanghellini, M. Tonini, S. Guerrini, C. Cremon, M. Degli Esposti, M. Koumandou, R. Corinaldesi, C. Sternini, and R. De Giorgio, *Neurology and neuropathology of the pancreatic innervation*. JOP, 2002. **3**(2): p. 26-33.
63. Rossi, J., P. Santamaki, M.S. Airaksinen, and K.H. Herzig, *Parasympathetic innervation and function of endocrine pancreas requires the glial cell line-*

- derived factor family receptor alpha2 (GFRalpha2)*. Diabetes, 2005. **54**(5): p. 1324-30.
64. el-Kamar, F.G., M.L. Grossbard, and P.S. Kozuch, *Metastatic pancreatic cancer: emerging strategies in chemotherapy and palliative care*. Oncologist, 2003. **8**(1): p. 18-34.
65. Marineo, G., *Untreatable pain resulting from abdominal cancer: new hope from biophysics?* JOP, 2003. **4**(1): p. 1-10.
66. Mercadante, S., E. Catala, E. Arcuri, and A. Casuccio, *Celiac plexus block for pancreatic cancer pain: factors influencing pain, symptoms and quality of life*. J Pain Symptom Manage, 2003. **26**(6): p. 1140-7.
67. Hwang, S.L., C.L. Lin, A.S. Lieu, T.H. Kuo, K.L. Yu, F. Ou-Yang, S.N. Wang, K.T. Lee, and S.L. Howng, *Punctate midline myelotomy for intractable visceral pain caused by hepatobiliary or pancreatic cancer*. J Pain Symptom Manage, 2004. **27**(1): p. 79-84.
68. Carroll, I., *Celiac plexus block for visceral pain*. Curr Pain Headache Rep, 2006. **10**(1): p. 20-5.
69. Ceyhan, G.O., C.W. Michalski, I.E. Demir, M.W. Muller, and H. Friess, *Pancreatic pain*. Best Pract Res Clin Gastroenterol, 2008. **22**(1): p. 31-44.
70. Farrar, J.T. and R.K. Portenoy, *Neuropathic cancer pain: the role of adjuvant analgesics*. Oncology (Williston Park), 2001. **15**(11): p. 1435-42, 1445; discussion 1445, 1450-3.
71. Pasero, C., *Pathophysiology of neuropathic pain*. Pain Manag Nurs, 2004. **5**(4 Suppl 1): p. 3-8.

72. Ceyhan, G.O., N.A. Giese, M. Erkan, A.G. Kersch, M.N. Wente, T. Giese, M.W. Buchler, and H. Friess, *The neurotrophic factor artemin promotes pancreatic cancer invasion*. *Ann Surg*, 2006. **244**(2): p. 274-81.
73. Ceyhan, G.O., I.E. Demir, U. Rauch, F. Bergmann, M.W. Muller, M.W. Buchler, H. Friess, and K.H. Schafer, *Pancreatic neuropathy results in "neural remodeling" and altered pancreatic innervation in chronic pancreatitis and pancreatic cancer*. *Am J Gastroenterol*, 2009. **104**(10): p. 2555-65.
74. Demir, I.E., G.O. Ceyhan, U. Rauch, B. Altintas, M. Klotz, M.W. Muller, M.W. Buchler, H. Friess, and K.H. Schafer, *The microenvironment in chronic pancreatitis and pancreatic cancer induces neuronal plasticity*. *Neurogastroenterol Motil*, 2010. **22**(4): p. 480-90, e112-3.
75. Bockman, D.E., M. Buchler, P. Malfertheiner, and H.G. Beger, *Analysis of nerves in chronic pancreatitis*. *Gastroenterology*, 1988. **94**(6): p. 1459-69.
76. Ceyhan, G.O., F. Bergmann, M. Kadihasanoglu, B. Altintas, I.E. Demir, U. Hinz, M.W. Muller, T. Giese, M.W. Buchler, N.A. Giese, and H. Friess, *Pancreatic neuropathy and neuropathic pain--a comprehensive pathomorphological study of 546 cases*. *Gastroenterology*, 2009. **136**(1): p. 177-186 e1.
77. Steele, F.R., G.J. Chader, L.V. Johnson, and J. Tombran-Tink, *Pigment epithelium-derived factor: neurotrophic activity and identification as a member of the serine protease inhibitor gene family*. *Proc Natl Acad Sci U S A*, 1993. **90**(4): p. 1526-30.
78. Becerra, S.P., A. Sagasti, P. Spinella, and V. Notario, *Pigment epithelium-derived factor behaves like a noninhibitory serpin. Neurotrophic activity does not require the serpin reactive loop*. *J Biol Chem*, 1995. **270**(43): p. 25992-9.

79. Barnstable, C.J. and J. Tombran-Tink, *Neuroprotective and antiangiogenic actions of PEDF in the eye: molecular targets and therapeutic potential*. Prog Retin Eye Res, 2004. **23**(5): p. 561-77.
80. Filleur, S., T. Nelius, W. de Riese, and R.C. Kennedy, *Characterization of PEDF: a multi-functional serpin family protein*. J Cell Biochem, 2009. **106**(5): p. 769-75.
81. Simonovic, M., P.G. Gettins, and K. Volz, *Crystal structure of human PEDF, a potent anti-angiogenic and neurite growth-promoting factor*. Proc Natl Acad Sci U S A, 2001. **98**(20): p. 11131-5.
82. Filleur, S., K. Volz, T. Nelius, Y. Mirochnik, H. Huang, T.A. Zaichuk, M.S. Aymerich, S.P. Becerra, R. Yap, D. Veliceasa, E.H. Shroff, and O.V. Volpert, *Two functional epitopes of pigment epithelial-derived factor block angiogenesis and induce differentiation in prostate cancer*. Cancer Res, 2005. **65**(12): p. 5144-52.
83. Tombran-Tink, J. and L.V. Johnson, *Neuronal differentiation of retinoblastoma cells induced by medium conditioned by human RPE cells*. Invest Ophthalmol Vis Sci, 1989. **30**(8): p. 1700-7.
84. Tombran-Tink, J., G.G. Chader, and L.V. Johnson, *PEDF: a pigment epithelium-derived factor with potent neuronal differentiative activity*. Exp Eye Res, 1991. **53**(3): p. 411-4.
85. Tombran-Tink, J., A. Li, M.A. Johnson, L.V. Johnson, and G.J. Chader, *Neurotrophic activity of interphotoreceptor matrix on human Y79 retinoblastoma cells*. J Comp Neurol, 1992. **317**(2): p. 175-86.
86. Tombran-Tink, J., K. Mazuruk, I.R. Rodriguez, D. Chung, T. Linker, E. Englander, and G.J. Chader, *Organization, evolutionary conservation,*

- expression and unusual Alu density of the human gene for pigment epithelium-derived factor, a unique neurotrophic serpin.* Mol Vis, 1996. **2**: p. 11.
87. Pignolo, R.J., V.J. Cristofalo, and M.O. Rotenberg, *Senescent WI-38 cells fail to express EPC-1, a gene induced in young cells upon entry into the G0 state.* J Biol Chem, 1993. **268**(12): p. 8949-57.
88. Tombran-Tink, J., S.M. Shivaram, G.J. Chader, L.V. Johnson, and D. Bok, *Expression, secretion, and age-related downregulation of pigment epithelium-derived factor, a serpin with neurotrophic activity.* J Neurosci, 1995. **15**(7 Pt 1): p. 4992-5003.
89. Francis, M.K., S. Appel, C. Meyer, S.J. Balin, A.K. Balin, and V.J. Cristofalo, *Loss of EPC-1/PEDF expression during skin aging in vivo.* J Invest Dermatol, 2004. **122**(5): p. 1096-105.
90. Taniwaki, T., S.P. Becerra, G.J. Chader, and J.P. Schwartz, *Pigment epithelium-derived factor is a survival factor for cerebellar granule cells in culture.* J Neurochem, 1995. **64**(6): p. 2509-17.
91. Sugita, Y., S.P. Becerra, G.J. Chader, and J.P. Schwartz, *Pigment epithelium-derived factor (PEDF) has direct effects on the metabolism and proliferation of microglia and indirect effects on astrocytes.* J Neurosci Res, 1997. **49**(6): p. 710-8.
92. Bilak, M.M., A.M. Corse, S.R. Bilak, M. Lehar, J. Tombran-Tink, and R.W. Kuncl, *Pigment epithelium-derived factor (PEDF) protects motor neurons from chronic glutamate-mediated neurodegeneration.* J Neuropathol Exp Neurol, 1999. **58**(7): p. 719-28.

93. Cao, W., J. Tombran-Tink, W. Chen, D. Mrazek, R. Elias, and J.F. McGinnis, *Pigment epithelium-derived factor protects cultured retinal neurons against hydrogen peroxide-induced cell death*. J Neurosci Res, 1999. **57**(6): p. 789-800.
94. Dawson, D.W., O.V. Volpert, P. Gillis, S.E. Crawford, H. Xu, W. Benedict, and N.P. Bouck, *Pigment epithelium-derived factor: a potent inhibitor of angiogenesis*. Science, 1999. **285**(5425): p. 245-8.
95. Doll, J.A., V.M. Stellmach, N.P. Bouck, A.R. Bergh, C. Lee, L.P. Abramson, M.L. Cornwell, M.R. Pins, J. Borensztajn, and S.E. Crawford, *Pigment epithelium-derived factor regulates the vasculature and mass of the prostate and pancreas*. Nat Med, 2003. **9**(6): p. 774-80.
96. Uehara, H., M. Miyamoto, K. Kato, Y. Ebihara, H. Kaneko, H. Hashimoto, Y. Murakami, R. Hase, R. Takahashi, S. Mega, T. Shichinohe, Y. Kawarada, T. Itoh, S. Okushiba, S. Kondo, and H. Kato, *Expression of pigment epithelium-derived factor decreases liver metastasis and correlates with favorable prognosis for patients with ductal pancreatic adenocarcinoma*. Cancer Res, 2004. **64**(10): p. 3533-7.
97. Hase, R., M. Miyamoto, H. Uehara, M. Kadoya, Y. Ebihara, Y. Murakami, R. Takahashi, S. Mega, L. Li, T. Shichinohe, Y. Kawarada, and S. Kondo, *Pigment epithelium-derived factor gene therapy inhibits human pancreatic cancer in mice*. Clin Cancer Res, 2005. **11**(24 Pt 1): p. 8737-44.
98. Erkan, M., C.W. Michalski, S. Rieder, C. Reiser-Erkan, I. Abiatari, A. Kolb, N.A. Giese, I. Esposito, H. Friess, and J. Kleeff, *The activated stroma index is a novel and independent prognostic marker in pancreatic ductal adenocarcinoma*. Clin Gastroenterol Hepatol, 2008. **6**(10): p. 1155-61.



99. Olive, K.P., M.A. Jacobetz, C.J. Davidson, A. Gopinathan, D. McIntyre, D. Honess, B. Madhu, M.A. Goldgraben, M.E. Caldwell, D. Allard, K.K. Frese, G. Denicola, C. Feig, C. Combs, S.P. Winter, H. Ireland-Zecchini, S. Reichelt, W.J. Howat, A. Chang, M. Dhara, L. Wang, F. Ruckert, R. Grutzmann, C. Pilarsky, K. Izeradjene, S.R. Hingorani, P. Huang, S.E. Davies, W. Plunkett, M. Egorin, R.H. Hruban, N. Whitebread, K. McGovern, J. Adams, C. Iacobuzio-Donahue, J. Griffiths, and D.A. Tuveson, *Inhibition of Hedgehog signaling enhances delivery of chemotherapy in a mouse model of pancreatic cancer*. Science, 2009. **324**(5933): p. 1457-61.
100. Megibow, A.J., *Pancreatic adenocarcinoma: designing the examination to evaluate the clinical questions*. Radiology, 1992. **183**(2): p. 297-303.
101. Kisker, O., C.M. Becker, D. Prox, M. Fannon, R. D'Amato, E. Flynn, W.E. Fogler, B.K. Sim, E.N. Allred, S.R. Pirie-Shepherd, and J. Folkman, *Continuous administration of endostatin by intraperitoneally implanted osmotic pump improves the efficacy and potency of therapy in a mouse xenograft tumor model*. Cancer Res, 2001. **61**(20): p. 7669-74.
102. Bernard, A., J. Gao-Li, C.A. Franco, T. Bouceba, A. Huet, and Z. Li, *Laminin receptor involvement in the anti-angiogenic activity of pigment epithelium-derived factor*. J Biol Chem, 2009. **284**(16): p. 10480-90.
103. Notari, L., V. Baladron, J.D. Aroca-Aguilar, N. Balko, R. Heredia, C. Meyer, P.M. Notario, S. Saravanamuthu, M.L. Nueda, F. Sanchez-Sanchez, J. Escribano, J. Laborda, and S.P. Becerra, *Identification of a lipase-linked cell membrane receptor for pigment epithelium-derived factor*. J Biol Chem, 2006. **281**(49): p. 38022-37.

104. Curtis, R., H.J. Stewart, S.M. Hall, G.P. Wilkin, R. Mirsky, and K.R. Jessen, *GAP-43 is expressed by nonmyelin-forming Schwann cells of the peripheral nervous system*. J Cell Biol, 1992. **116**(6): p. 1455-64.
105. Sensenbrenner, M., M. Lucas, and J.C. Deloulme, *Expression of two neuronal markers, growth-associated protein 43 and neuron-specific enolase, in rat glial cells*. J Mol Med, 1997. **75**(9): p. 653-63.
106. Ceyhan, G.O., F. Bergmann, M. Kadihasanoglu, M. Erkan, W. Park, U. Hinz, T. Giese, M.W. Muller, M.W. Buchler, N.A. Giese, and H. Friess, *The neurotrophic factor artemin influences the extent of neural damage and growth in chronic pancreatitis*. Gut, 2007. **56**(4): p. 534-44.
107. Petersen, S.V., Z. Valnickova, and J.J. Enghild, *Pigment-epithelium-derived factor (PEDF) occurs at a physiologically relevant concentration in human blood: purification and characterization*. Biochem J, 2003. **374**(Pt 1): p. 199-206.
108. Luttenberger, T., A. Schmid-Kotsas, A. Menke, M. Siech, H. Beger, G. Adler, A. Grunert, and M.G. Bachem, *Platelet-derived growth factors stimulate proliferation and extracellular matrix synthesis of pancreatic stellate cells: implications in pathogenesis of pancreas fibrosis*. Lab Invest, 2000. **80**(1): p. 47-55.
109. Tombran-Tink, J. and C.J. Barnstable, *Therapeutic prospects for PEDF: more than a promising angiogenesis inhibitor*. Trends Mol Med, 2003. **9**(6): p. 244-50.
110. Zhu, Z., H. Friess, F.F. diMola, A. Zimmermann, H.U. Graber, M. Korc, and M.W. Buchler, *Nerve growth factor expression correlates with perineural*

- invasion and pain in human pancreatic cancer. J Clin Oncol, 1999. 17(8): p. 2419-28.*
111. Bockman, D.E., M. Buchler, and H.G. Beger, *Interaction of pancreatic ductal carcinoma with nerves leads to nerve damage. Gastroenterology, 1994. 107(1): p. 219-30.*
  112. Baloh, R.H., M.G. Tansey, E.M. Johnson, Jr., and J. Milbrandt, *Functional mapping of receptor specificity domains of glial cell line-derived neurotrophic factor (GDNF) family ligands and production of GFRalpha1 RET-specific agonists. J Biol Chem, 2000. 275(5): p. 3412-20.*
  113. Ceyhan, G.O., S. Deucker, I.E. Demir, M. Erkan, M. Schmelz, F. Bergmann, M.W. Muller, T. Giese, M.W. Buchler, N.A. Giese, and H. Friess, *Neural fractalkine expression is closely linked to pain and pancreatic neuritis in human chronic pancreatitis. Lab Invest, 2009. 89(3): p. 347-61.*
  114. Ceyhan, G.O., I.E. Demir, B. Altintas, U. Rauch, G. Thiel, M.W. Muller, N.A. Giese, H. Friess, and K.H. Schafer, *Neural invasion in pancreatic cancer: a mutual tropism between neurons and cancer cells. Biochem Biophys Res Commun, 2008. 374(3): p. 442-7.*
  115. Houenou, L.J., A.P. D'Costa, L. Li, V.L. Turgeon, C. Enyadike, E. Alberdi, and S.P. Becerra, *Pigment epithelium-derived factor promotes the survival and differentiation of developing spinal motor neurons. J Comp Neurol, 1999. 412(3): p. 506-14.*

## 8. CURRICULUM VITAE

**Family Name:** Samkharadze  
**First Name:** Tamar  
**Date of birth:** October 30, 1981  
**Nationality:** Georgian  
**Present Address:** Rablstrasse 12, 81669, Munich, Germany  
**Tel:** +(49) 017675597443  
**E-mail:** samkharadze.tamar@googlemail.com

### EDUCATION:

September 1988 – June 1999: Primary School, Tbilisi, Georgia

September 1999 – June 2005: "AIETI" Medical School, Tbilisi, Georgia

### PROFESSIONAL EXPERIENCE:

July 2005 - August 2006: Medical Doctor, "Medulla - Chemotherapy and Immunotherapy Clinic", Tbilisi, Georgia

March 2006 – October 2006: Manager, Site Management Organization - "Pharmina", Tbilisi, Georgia

October 2006 – November 2007: Clinical Research Associate, Clinical Research Organization "MB Quest, Inc.", Tbilisi, Georgia

November 2007 – present: Fellow of the Research group of PD Dr. Jörg Kleeff, Department of General Surgery, Klinikum Rechts der Isar, Technische Universität München, Munich, Germany

## **PUBLISHED PAPERS:**

Erkan M, Weis N, Pan Z, Schwager C, **Samkharadze T**, Jiang X, Wirkner U, Giese NA, Ansorge W, Debus J, Huber PE, Friess H, Abdollahi A, Kleef J. (2010). "Organ-, inflammation- and cancer specific transcriptional fingerprints of pancreatic and hepatic stellate cells". *Mol Cancer*. Apr 23; 9:88.

**Samkharadze T**, Erkan M, Reiser-Erkan C, Demir IE, Kong B, Ceyhan GO, Michalski CW, Esposito I, Friess H, Kleeff J. (2011). "Pigment Epithelium-Derived Factor Associates With Neuropathy and Fibrosis in Pancreatic Cancer". *Am J Gastroenterol*. Jan 11; [Epub ahead of print]

## **9. ACKNOWLEDGEMENTS:**

I owe a lot to many people whom I had the pleasure of meeting during my scientific fellowship.

I am grateful to Professor Helmut Friess for giving me a chance to conduct the basic research and develop my scientific career in the field of pancreatic cancer at the Technische Universität München.

I especially want to thank Dr. Jörg Kleeff for his supervision and patience. Without his guidance and support my scientific work would not have been successful. It was my pleasure to be a member of his research team.

I would like to sincerely thank my supervisor Dr. Mert Erkan for his mentorship, friendship, understanding and guidance. This thesis would not have been even possible without his efforts of explaining things clear and easy way. I will never forget his support through these years, especially during my first days in the lab.

Huge thanks to Dr. Christoph Michalski for scientific and social support, for creation of the friendly environment at work and for everything he has done for me.

I would like to thank all my lab-mates and colleagues for helping me their own special ways, for encouragement, helpful advices and for the precious moments we shared. I especially want to thank Dr. Ivane Abiatari for his friendship, help through the difficult times and for emotional support.

Finally, my special thanks to my family. The words can not express how grateful I am to my parents and my brother for believing in me, for encouraging me to be myself holding my hand and sharing all my success and failure with me.